

Two-dimensional IFIR Structures Using Generalized Factorable Filters

Roberto Manduchi¹
University of California at Berkeley
Computer Science Division
Technical Report UCB//CSD-93-785

October 7, 1994

¹This work was supported by a fellowship offered by the Associazione Elettrotecnica Italiana (A.E.I.), Italy

Abstract

The extension of the idea of Interpolated FIR filters to the two-dimensional case is presented. Such systems allow for lower computational weight, in terms of number of elementary operations per input sample. In the 1-D case, the justification to such a performance advantage rests upon the relationship between filter order, transition bandwidth and minimax errors for equiripple linear-phase filters. Even though no similar relation is known for minimax optimal multidimensional filters, a qualitatively parallel behaviour is shared by a class of suboptimal filters recently developed by Chen and Vaidyanathan. Such filters are particularly suitable for the sampling structure conversion of video signals. In particular, they belong to the class of Generalized Factorable filters, for which an efficient implementation exists.

We examine in detail the design procedure of Generalized Factorable filters, and devise some properties that have not been described before in the literature. Then, we apply such filter in the 2-D IFIR scheme.

An interesting problem peculiar to the multidimensional case is the choice of the sublattice which represents the definition support of the first-stage filter. We present a strategy to choose (given the spectral support of the desired frequency response) the optimal sublattice, and to design the second-stage (interpolator) filter in order to achieve low overall computational complexity.

Chapter 1

Introduction

Interpolated finite impulse response (IFIR) filters have been introduced by Neuvo, Dong and Mitra [1]. In its simplest form, an IFIR structure is an FIR filter whose transfer function can be written as¹

$$H(z) = \bar{F}(z^L) G(z) \quad (1.1)$$

where $\bar{F}(\cdot)$ and $G(\cdot)$ are polynomials and L is some integer. In other words, an IFIR filter is the cascade of two FIR filters ($f(n)$, the *shaping* filter, and $g(n)$, the *interpolator* filter), with $f(n) \neq 0$ only if n is a multiple of L (then $\bar{f}(n) = f(Ln)$).

IFIR filters are interesting because they can be implemented efficiently. The number of elementary operations (multiplications or sums) per input sample (called OPS) required to implement an FIR filter is approximately equal to the number N of non-null coefficients of its impulse response². Hence, if $N_{\bar{f}}$ is the length of $\bar{f}(n)$, and N_g is the length of $g(n)$, approximately $N_{\text{IFIR}} = N_{\bar{f}} + N_g$ OPS's are required to implement the IFIR structure (in spite of the fact that the length of $f * g(n)$ is $(L - 1)N_{\bar{f}} + N_g > N_{\text{IFIR}}$ if $L > 1$). The minimum length N_h of an FIR filter $h(n)$ to meet some prescribed specifics is, for certain classes of filters (e.g., minimax low-pass with narrow pass-band and transition band), larger than N_{IFIR} relative to a suitable IFIR structure satisfying the same specifications. Hence, IFIR filters allow for computational savings in such cases. However, the number of memory cells required for the implementation of the IFIR structure is $N_f + N_g - 2$, which is typically slightly larger than $N_h - 1$ (the number of elementary cells required to realize $h(n)$).

Expression (1.1) is reminiscent of the polyphase decomposition of an FIR filter into its generalized form [2],[3]. As a matter of fact, an IFIR filter is a special case of FIR filter, which admits an L -fold generalized polyphase decomposition constituted by a single branch [2]. Another interesting aspect of IFIR filters theory, is the connection with the multistage implementation of interpolators and decimators [4],[5]. One can easily show (using an elementary property of multirate systems, expressed by the “noble identities” [2]) that the interpolation or decimation using an IFIR filter can be implemented by the multistage (multirate) scheme of Crochiere and Rabiner (see Fig. 1.1). The two structures are formally equivalent: the theory developed for the multistage sampling structure conversion ([4],[5]) can be used to design IFIR filters, and vice-versa.

The IFIR filters that have been considered in the literature, were intended to approximate ideal low-pass or band-pass frequency response in a minimax sense [1],[6],[7]. The impulse response of an IFIR filter can be regarded to as the interpolated version of a “decimated” one. Because the impulse response of selective band optimal FIR filters is typically highly correlated, it is intuitive that a “simple” interpolator should be able to fulfill the purpose. A quantitative analysis of such

¹We will always denote by a capital letter the transfer function or the frequency response of a system whose impulse response is denoted by the corresponding small letter.

²Actually, in a direct form realization, the number of multiplications is N ($(N + 1)/2$ if zero-phase), while the number of sums is $N - 1$.

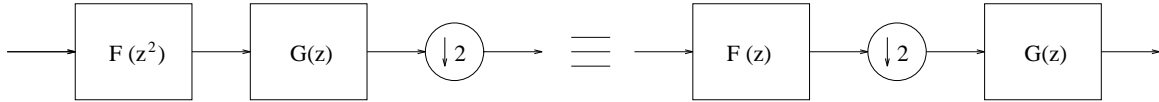


Figure 1.1: Proof of the equivalence of IFIR structure and multistage decimation.

a notion can be carried out by exploiting the (approximate) analytical relation which holds among the parameters of a minimax filter (filter length N , pass-band and stop-band frequencies f_p and f_s , pass-band and stop-band ripples δ_p and δ_s) for small ripples δ_p and δ_s [8],[9]:

$$N \propto \frac{20 \log(\delta_p \delta_s) - 13}{f_s - f_p} \quad (1.2)$$

The important characteristic of relation (1.2) is that, for sufficiently large N , the transition bandwidth ($f_s - f_p$) is approximately inversely proportional to N (for fixed product $\delta_p \delta_s$).

The previous observations suggested the original simple design technique (proposed, for multistage interpolation-decimation schemes, in [4], and for IFIR filters in [1]), where the shaping and the interpolator filters were designed independently of each other. The amount of the pass-band and of the stop-band ripples of the overall filter depends on the relative positions of the oscillations of the frequency responses of $f(n)$ and $g(n)$, which are unknown in general. Hence, only upper bounds for the resulting δ_p and δ_s are predictable. If δ_p^f and δ_s^f are the pass-band and stop-band ripples of the shaping filter, and δ_p^g and δ_s^g those of the interpolator, from (1.1) one has:

$$\delta_p \leq \delta_p^f + \delta_p^g + \delta_p^f \delta_p^g \simeq \delta_p^f + \delta_p^g \quad (1.3)$$

$$\delta_s \leq \max(\delta_s^f, \delta_s^g + \delta_p^f \delta_s^g) \simeq \max(\delta_s^f, \delta_s^g) \quad (1.4)$$

Such worst-case relations can be exploited for the choice of the specifics of the shaping filter and of the interpolator, to achieve desired maximum values δ_p and δ_s , as in [4]. If optimal minimax filters are used, the required filter orders can be obtained using the relations presented in [8],[9],[10]. Note that, although in their original work [1], Neuvo, Dong and Mitra suggested the use of a simple first-order or second-order interpolator, higher order interpolators can be used profitably, as in [6].

Since relations (1.3) and (1.4) represent upper bounds for the overall ripples, choosing pass-band and stop-band ripples for $f(n)$ and $g(n)$ such that (1.3) and (1.4) are satisfied as equalities leads, in most cases, to overall ripples smaller than required. The designer can then try different choices for the shaping filter and the interpolator, allowing the parameters $\delta_p^f, \delta_s^f, \delta_p^g, \delta_s^g$ to increase (therefore decreasing the corresponding filter lengths), until a satisfactory result is found. The IFIR filters designed by means of such a heuristic procedure are in general not optimal, and a certain experience of the designer is required. On the other side, the method is simple and straightforwardly extendible to the multidimensional case, as described in the present work.

Several improvements to the simple design procedure just described have been proposed. Crochiere and Rabiner early realized that adopting multiple stop-band (instead of single stop-band) interpolator filters, can provide fairly significant filter order reduction [11]. Such an idea was generalized by Saramäki, Neuvo and Mitra [6] to obtain equiripple behaviour of the overall IFIR filter frequency response. They proposed a procedure to iteratively design $\bar{F}(z^L)$ and $G(z)$ using the Remez exchange algorithm. Their method allows to design optimal (in a minimax sense) IFIR filters; however, it is not clear how to find a multidimensional version of such a technique.

The theory of multidimensional (M-D) multistage sampling structure conversion has been first proposed by Ansari and Lee [12] and by Chen and Vaidyanathan [13] first, and then developed in some extent by Manduchi, Cortelazzo and Mian [14]. Also in the multidimensional case, the theory of multistage sampling structure conversion and of IFIR filters are equivalent, and we will

deal only with IFIR filter hereinafter. For the sake of simplicity, only 2-D domains will be studied in this work. The results can be extended to higher dimensions without major difficulties.

The task here is to design a 2-D filter, defined on a given lattice Λ , whose frequency response approximates some desired function $D(\mathbf{f})$. The simplest IFIR scheme is composed by the cascade of a shaping filter, whose coefficient are not null only on a sublattice Λ_L (L times less dense than Λ), and of the interpolator filter. While in [12] and in [13] the necessary conditions (in terms of sampling lattices and spectral support determination) for a multistage scheme - IFIR structure are stated, and in [14] a simple design example is given, no serious attempt to produce efficient 2-D IFIR filters defined on a given sampling lattice have been proposed in the literature. The purpose of this work is to provide a framework for the design of such systems, for a certain class of frequency response shapes widely used in video technology.

The principal novelties of 2-D IFIR filters with respect to the 1-D case are:

1. M-D sampling lattices admit more than just one sublattice for a given decimation ratio [15],[16];
2. The frequency response of M-D filters cannot be easily characterized as in the 1-D case; in other words, a pass-band or a stop-band region can exhibit any shape (while in the case of low-pass 1-D, they are bound to be segments).

Observation 1 leads to the following problem: given a decimation index L , which sublattice of definition of the coefficients of the shaping filter is more suitable for a given $D(\mathbf{f})$? The determination of all the sublattices for a given density ratio has been analyzed in [16], and an application to multistage sampling structure conversion (via the idea of *lattice chains*, see also [17]) has been described in [14]. In the present work, it will be shown that, given the desired frequency response mask, certain sublattices allow for the easy interpolation of the samples of the shaping filter, while other ones make the interpolation extremely difficult.

The spectral support of a 2-D filter may assume any shape, and devising a general technique for the IFIR system design seems an overwhelming task. Fortunately, for a large variety of applications, only frequency responses belonging to particular classes are of interest. For example, frequency responses with pass-band in the shape of a parallelogram (typically a diamond) are suitable for the sampling structures conversion of video signals [15],[18],[14], as well as for a variety of other applications. We will concentrate in this work on such a class of spectral masks.

In the procedure we propose, the design of the shaping filter and of the interpolator are carried out separately. As in the 1-D case, given the subsampling factor L , a worst case analysis provides specifics for the two filters to be used as a starting point. Then, one can move around the space of filter parameters for any of the two filters (note that the filter masks are easily parametrized, as they are parallelograms). As mentioned above, a new parameter to take care of is the sublattice of definition of the shaping filter.

In order to apply such a procedure efficiently, it is necessary that the filter design technique be fast and easy to use. It should give the designer the control of the frequency response parameters, as well as of the impulse response size. The possibility of efficient implementation, typical of certain classes of 2-D filters, is an important bonus to take into account.

Several design techniques for 2-D filters have been proposed in the literature. Optimal minimax 2-D filter can be designed via iterative procedures similar to the Remez exchange algorithm [19],[20] or via linear programming [21],[22],[23]. In particular, linear programming allows to include linear constraints on the filter coefficients (e.g., “antiringing” constraints on the step response [23]). Filters designed via linear programming have been employed for the multistage sampling conversion scheme of [14]. However, such a design technique (besides being computationally very intensive) does not offer efficient implementative schemes.

2-D FIR filters designed by frequency transformation [24] have received a lot of attention, because they derive from 1-D filters (which are well understood), can be optimal (starting from optimal 1-D filters) in certain cases [25], and possess an efficient implementation [26]. However,

tuning the design parameters in order to obtain diamond-shaped frequency responses mask, however, is somewhat cumbersome [27]. In plus, little control on the impulse response (beside the side of the square which represents its support) is achievable.

The filter design technique we have chosen for our system, is the one recently proposed by Chen and Vaidyanathan in [13],[28]. We will call the resulting filters “generalized factorable” (GF) for reasons that will be clear in Section 2. GF filters are designed starting from two suitable 1-D filters, taking the tensor product of their impulse responses, subsampling it on a suitable sublattices of Z^2 , and finally reordering the samples on the desired definition lattice. The main advantages of GF filters are:

1. They “naturally” provide spectral supports in the shape of parallelograms;
2. The design procedure is very fast (the computational burden is due to the design of two 1-D filters) and simple, lending itself to use in automatic design systems (CAD);
3. They admit an efficient “generalized factorable” implementation, which can reduce effectively the computational weight;
4. It is possible to control the size and some characteristics of the impulse response.

A drawback of the GF filter design technique is that, starting from 1-D optimal minimax filters, one does not get optimal minimax 2-D filters. Nevertheless, they exhibit the interesting property that approximate (worst case) relations can be found among the filter parameters of interest (filter size, transition region, pass-band and stop-band ripples). Exploiting such relations it is possible to predict lower bounds on the performance attainable by 2-D IFIR filters, like in the 1-D case. It is interesting to note that similar relations have been described in the literature also for other classes of filters (circularly symmetric filters from 1-D prototypes [26] and diamond-shaped minimax filters [23]).

In our scheme, GF filters are used both for the shaping filter and the interpolator. A nice feature provided by the algorithm, is that it gives a simple geometrical characterization of the filters’ frequency response supports, which makes them easily tractable. Following our algorithm, all feasible sublattices of definition of the coefficients of the shaping filter are tested. For each of them, the “best” shapes for the interpolator filters are chosen. This procedure can be implemented in a completely automatic fashion. Then, it is up to the designer choosing the combination sublattice-interpolator which best satisfies the design constraints.

In the experimental section, we have considered both the non-factorable and the generalized factorable implementations for the filters. In this way, we provide a reasonable estimate of the system’s performance when other filters than GF are employed. The results show that, in the non-factorable case, improvements in terms of computational weight, comparable to the 1-D case, are achievable, depending on the shape and on the size of the pass-band and of the stop-band regions. Interestingly enough, the situation is not as simple using the generalized factorable implementation. It is shown that, depending on the geometry of the decimation lattices (which, in turn, depend on the shape of the spectral support), an IFIR structure may or may not lead to the reduction of the overall computational weight.

The paper is organized as follows. Section 2 reviews the theory of GF filters. With respect to the original work by Chen and Vaidyanathan [13], the formalism has been slightly changed, the algorithm has been stated in a more comprehensive fashion, and some new results, regarding symmetries and frequency response and step response properties, have been added. Section 3 describes the proposed IFIR design procedure and shows the experimental examples. Section 4 has the conclusions. In order to make the paper self-contained, some non-standard notions regarding multidimensional sampling structures (some of which are original contribution of this work), as well as the adopted nomenclature, are reported in Appendix A. In Appendix B, formal definitions (both for the 1-D and the 2-D case) of certain useful filter parameters are provided. Appendix C contains the proof of a result used in Section 2.3.3, regarding some properties of the step response of ideal filters.

Chapter 2

Generalized Factorable Filters

In this section, we review the algorithm proposed by Chen and Vaidyanathan [13],[28] to design 2-D filters with pass-band in the shape of a parallelepiped. It will be seen in Section 2.2 that the resulting filters actually belong to the general class of generalized factorable (GF) filters. A number of features that make such filters appealing for use in an IFIR structure, have been listed in the Introduction. In Section 2.1 we briefly restate the algorithm, and in Section 2.2 we define the general class of generalized factorable filters. In Subsection 2.3 we study certain properties of GF filters, that have not been described before in the literature. Throughout the whole section, we make extensive use of the formalism and of the basic results of Appendices A and B.

2.1 Chen and Vaidyanathan's Design Technique for 2D Filters

Consider a sampling lattice $\Lambda = LAT(\mathbf{C})$. The procedure proposed by Chen and Vaidyanathan [13],[28] enables to design an M-D FIR filter defined on Λ , with pass-band region approximating a parallelepiped centered in the origin, starting from M suitable 1-D low-pass filters.

Let

$$Par(\mathbf{P}) = \left\{ \sum_{i=1}^M \alpha_i \mathbf{p}_i, -1 \leq \alpha_i \leq 1 \right\} \quad (2.1)$$

be a parallelepiped (representing the desired pass-band region), characterized by matrix $\mathbf{P} = (\mathbf{p}_1 | \mathbf{p}_2 | \dots | \mathbf{p}_M)$. We assume that \mathbf{P} has only rational entries. Consider the parallelepiped $Par(\mathbf{P}_t) = \mathbf{C}^T \mathbf{P}$ (matrix \mathbf{C} can be any basis of Λ). $Par(\mathbf{P}_t)$ represents a “transformed” version of the pass-band region $Par(\mathbf{P})$. Let

$$\bar{\mathbf{A}} = \mathbf{P}_t^T \text{den}(\mathbf{P}_t) \in Z_M \quad (2.2)$$

Now consider filter $\bar{h}(\mathbf{n}) = \prod_{i=1}^M q(n_i)$, where $q(n)$ is an ideal 1-D filter such that

$$Q(f) = \begin{cases} 1 & , |f| \leq f_p \\ 0 & , f_p < |f| \leq 0.5 \end{cases} \quad (2.3)$$

and $f_p = 1/\text{den}(\mathbf{P}_t)$. Filter $\hat{h}(\mathbf{n}) = |\det(\bar{\mathbf{A}})| \bar{h}(\bar{\mathbf{A}}\mathbf{n})$ is such that, within a suitable elementary cell,

$$\bar{H}(\mathbf{f}) = \begin{cases} 1 & , \mathbf{f} \in Par(\mathbf{P}_t) \\ 0 & , \text{otherwise} \end{cases} \quad (2.4)$$

The just described algorithm suffers from a “design overhead” [28], in the sense that $|\det(\bar{\mathbf{A}})|$ (the “decimation ratio”) is typically higher than necessary, and filter $Q(f)$ may have a very narrow

transition band. It is important that $|\det(\mathbf{A})|$ be small for the control of the filter characteristics, as will be stressed later in Section 2.3.6. It is possible (in general) to lower such a value by allowing for different 1-D filters along the axes. Let

$$\tilde{\mathbf{A}} = \mathbf{D}\mathbf{A} \quad , \quad \mathbf{D} = \text{diag}(d_1, d_2, \dots, d_M) \quad (2.5)$$

where d_i is the largest integer that divides each entry of the i -th row of $\tilde{\mathbf{A}}$. Note that $\mathbf{A} \in Z_M$. Consider M 1-D ideal filters $q_i(n)$, such that

$$Q_i(f) = \begin{cases} 1 & , \quad |f| \leq f_{p_i} \\ 0 & , \quad f_{p_i} < |f| \leq 0.5 \end{cases} \quad (2.6)$$

where $f_{p_i} = d_i/\text{den}(\mathbf{P}_t)$. Their tensor product

$$\bar{h}(\mathbf{n}) = \prod_{i=1}^M q_i(n_i) \quad (2.7)$$

has spectral support in $Par(\text{diag}(f_{p_1}, f_{p_2}, \dots, f_{p_M}))$, while $\hat{h}(\mathbf{n}) = |\det(\mathbf{A})| \cdot \bar{h}(\mathbf{A}\mathbf{n})$ has spectral support in $Par(\mathbf{P}_t)$. Finally, the sought for filter $h(\mathbf{C}\mathbf{n})$ such that, within a suitable elementary cell of Λ^* , it is

$$H(\mathbf{f}) = \begin{cases} 1 & , \quad \mathbf{f} \in Par(\mathbf{P}) \\ 0 & , \quad \text{otherwise} \end{cases} \quad (2.8)$$

is given by

$$h(\mathbf{C}\mathbf{n}) = \hat{h}(\mathbf{n}) = |\det(\mathbf{A})| \bar{h}(\mathbf{A}\mathbf{n}) \quad (2.9)$$

Observations

1. In the original algorithm by Chen and Vaidyanathan [28], the authors used term $|\det(\mathbf{M})|$ (where $\mathbf{L}^{-1}\mathbf{M}$ is any left coprime factorization of \mathbf{P}_t) instead of term $\text{den}(\mathbf{P}_t)$ in (2.2). Such a choice yields higher values of $|\det(\tilde{\mathbf{A}})|$ than necessary, as $|\det(\mathbf{M})|$ can be larger than $\text{den}(\mathbf{P}_t)$ (for a proof, see the Appendix of [14]). However, if we allow the 1-D filters to differ from one another (like in the second part of the algorithm), any common factor in the entries of $\tilde{\mathbf{A}}$ will be “absorbed” by matrix \mathbf{D} .
2. Note that, from (2.9), any different choice $\tilde{\mathbf{C}} = \mathbf{C}\mathbf{U}$, unimodular \mathbf{U} , of basis of Λ , induces a different sampling matrix $\tilde{\mathbf{A}} = \mathbf{A}\mathbf{U}$.
3. In practical cases, filters $h_i(n)$ will be characterized by parameters $(f_{p_i}, f_{s_i}, \delta_{p_i}, \delta_{s_i}, N_i)$. Assume that the desired frequency response of filter $H(\mathbf{f})$ is specified by pass-band and stop-band surfaces $Par(\mathbf{P}_p)$ and $Par(\mathbf{P}_s)$ in the shape of parallelepipeds having pairwise parallel faces, i.e.,

$$\mathbf{P}_s = \mathbf{P}_p \mathbf{T} \quad , \quad \mathbf{T} = \text{diag}(t_1, t_2, \dots, t_n) \quad , \quad t_i > 1 \quad (2.10)$$

The related decimation matrices \mathbf{A}_p and \mathbf{A}_s computed following the previous algorithm may differ from each other. One way to circumvent such a problem, is to compute matrix \mathbf{A}_s and stop-band frequencies $\{f_{s_i}\}$ following the previous algorithm, impose $\mathbf{A}_p = \mathbf{A}_s \stackrel{\text{def}}{=} \mathbf{A}$, and set the pass-band frequencies $\{f_{p_i} = f_{s_i}/t_i\}$.

4. It is readily seen that

$$H(\mathbf{f}) = \sum_{\mathbf{r} \in P(LAT(A^T), Z^2)} \bar{H}(\mathbf{A}^{-T}(\mathbf{C}^T \mathbf{f} + \mathbf{r})) \quad (2.11)$$

and that the support of the impulse response of $h(\mathbf{Cn})$ is

$$Par\left(\mathbf{CA}^{-1}\text{diag}\left(\left\{\frac{N_i+1}{2}\right\}\right)\right)\cap\Lambda\quad(2.12)$$

where N_i is the length of the i -th 1-D filter in (2.6). In the following of this work, we will approximate the conventional length of $h(\mathbf{Cn})$ with $\left(\prod_{i=1}^M N_i\right)/|\det(\mathbf{A})|$.

5. Matrix \mathbf{D} in decomposition (2.5) has the following geometrical interpretation: $LAT(\mathbf{D})$ is the least dense factorable lattice (L.D.F.L., see Appendix A) containing $LAT(\tilde{\mathbf{A}})$. Then the L.D.F.L. containing $LAT(\mathbf{A})$ is Z^2 . This in turn implies that, if \mathbf{A} is diagonal, then $\mathbf{A} = \mathbf{I}$.
6. Suppose one is given a GF filter $h(\mathbf{a})$ defined on $\Lambda = LAT(\mathbf{C})$ with spectral support approximating $Par(\mathbf{P})$. Let $\Lambda_1 = LAT(\mathbf{CH})$ be a sublattice of Λ , and assume that the spectral support of $h(\mathbf{a})$ is contained within some elementary cell of Λ_1^* . In order to design a filter $g(\mathbf{a})$ with the same spectral support of $h(\mathbf{a})$, one can choose between two procedures. The simpler one is derived immediately from equation (2.9), letting $g(\mathbf{CHn}) = |\det(\mathbf{H})| h(\mathbf{CHn})$, i.e. subsampling $h(\mathbf{a})$ on Λ_1 . The conventional length N_g of $g(\mathbf{a})$ will be approximately equal to the conventional length N_h of $h(\mathbf{a})$, divided by $|\det(\mathbf{H})|$. If the L.D.F.L. containing $LAT(\mathbf{AH})$ is less dense than $LAT(\mathbf{D})$ (see Observation 5 above), one can employ the second part of the algorithm instead, and construct the new sampling matrix and the new pass-band and stop-band frequencies for the 1-D filters. It is easily seen (making use of relation (1.2)) that, if the 1-D filters are forced to exhibit the same pass-band and stop-band ripples as in the design of $h(\mathbf{a})$, the conventional length of $g(\mathbf{a})$ will be again approximately equal to $N_h/|\det(\mathbf{H})|$.

2.1.1 Generalized factorable implementation

A filter designed using the algorithm of Chen and Vaidyanathan is obtained by sampling an appropriate factorable impulse response. Hence, it should not be surprising that techniques for its efficient implementation can be devised. Let N_1 and N_2 be the lengths of the 1-D filters $q_1(n)$ and $q_2(n)$ (for the sake of notation's simplicity, in this section we will refer only to the 2-D case). If the filter $h(\mathbf{a})$ is implemented in direct form, approximately $N_1 N_2 / |\det(\mathbf{A})|$ OPS's are required. Chen and Vaidyanathan cleverly proved in [28] that it is possible to implement the filter performing only approximately $N_1 + N_2$ OPS's. Their proof is based on a machinery of formal identities. We give here a (hopefully) more intuitive proof, which will turn out to be useful when dealing with IFIR structures. In the effort to be clear we will divide the proof in several steps.

Let \mathbf{C} and \mathbf{A} be bases of the signal definition lattice and of the decimation lattice respectively, as in Section 2.1. Assume, without loss of generality, that \mathbf{A} is in upper Hermite normal form.

Step 1. Consider a change of basis on the input signal $x(\mathbf{Cn})$ and on filter $h(\mathbf{Cn})$:

$$\bar{x}(\mathbf{An}) = x(\mathbf{Cn}), \quad \bar{h}(\mathbf{An}) = h(\mathbf{Cn})\quad(2.13)$$

Step 2. Filter $\bar{h}(\mathbf{An})$ is not factorable (unless \mathbf{A} is unimodular), but it is made up of factorable polyphase components. To prove this, let $\mathbf{AH} = \text{diag}(S_1, S_2)$ be a basis of the densest factorable sublattice (D.F.S.) of $LAT(\mathbf{A})$. Then there are $\text{den}(A_{1,2}/A_{1,1})$ \mathbf{AH} -polyphase components in $\bar{h}(\mathbf{An})$:

$$\bar{h}^r(\mathbf{AHn}) \stackrel{\text{def}}{=} \bar{h}(\mathbf{AHn} + \mathbf{r}), \quad \mathbf{r} \in P(LAT(\mathbf{AH}), LAT(\mathbf{A}))\quad(2.14)$$

It is easy to see that each $\bar{h}^r(\mathbf{a})$, $\mathbf{a} \in LAT(\mathbf{AH})$, is factorable. In fact, let $\mathbf{a} = (k_1 S_1, k_2 S_2)^T$ and $\mathbf{r} = (r_1, r_2)^T$. Then

$$\bar{h}^r(\mathbf{a}) = q_1^{r_1}(k_1) q_2^{r_2}(k_2)\quad(2.15)$$

where q_i^s is the s -th S_i -polyphase component of filter $q_i(n)$:

$$q_i^s(n) \stackrel{\text{def}}{=} q_i(nS_i + s), \quad 0 \leq s < S_i \quad (2.16)$$

Step 3. At this point, it should be clear that the filtering of $\bar{x}(\mathbf{a})$ with $\bar{h}(\mathbf{a})$ can be done in a factorable fashion. It just needs to write down the \mathbf{AH} -polyphase decomposition of $\bar{h}(\mathbf{a})$ to get

$$\bar{X}(\mathbf{f})\bar{H}(\mathbf{f}) = \bar{X}(\mathbf{f}) \sum_{\mathbf{r}} e^{-j2\pi\mathbf{f}^T \mathbf{r}} \bar{H}^r(\mathbf{f}) = \sum_{\mathbf{r}} \left(\bar{X}(\mathbf{f})e^{-j2\pi\mathbf{f}^T \mathbf{r}} \right) \bar{H}^r(\mathbf{f}) \quad (2.17)$$

Each term $\left(\bar{X}(\mathbf{f})e^{-j2\pi\mathbf{f}^T \mathbf{r}} \right) \bar{H}^r(\mathbf{f})$ represents the (factorable) filtering by the \mathbf{r} -th polyphase component of $\bar{h}(\mathbf{a})$ of a version of $\bar{x}(\mathbf{a})$ displaced by \mathbf{r} .

It is interesting deriving the number of OPS's required for the implementation. Let the length of the two 1-D filters $q_1(n)$ and $q_2(n)$ be N_1 and N_2 respectively. Then the lengths of their polyphase components as in (2.16) are approximately N_1/S_1 and N_2/S_2 . Now, from Appendix A one has that the number of polyphase components is

$$\text{den}(A_{1,2}/A_{1,1}) = S_1/R_1 = S_2/R_2 \quad (2.18)$$

where $\text{diag}(R_1, R_2)$ is a basis of the L.D.F.L. containing $LAT(\mathbf{A})$. But, according to Observation 5 of Section 2.1, $R_1 = R_2 = 1$, and therefore $\text{den}(A_{1,2}/A_{1,1}) = S_1 = S_2$. Hence, the number of OPS's required is $N_1 + N_2$.

Consider now the case of a filter defined on a sublattice $\Lambda_1 = LAT(\mathbf{AH})$, designed by subsampling $h(\mathbf{a})$ (as in the first procedure of Observation 6 above). Let $\text{diag}(R'_1, R'_2)$ be a basis of the L.D.F.L. containing $LAT(\mathbf{AH})$, and let $\mathbf{AH}' = \text{diag}(S'_1, S'_2)$ be the D.F.S. of $LAT(\mathbf{AH})$ (note that $S'_1 \geq S_1, S'_2 \geq S_2$). Then there are $S'_1/R'_1 = S'_2/R'_2$ polyphase components along the i -th axis, each one of length N_i/S'_i approximately. The number of OPS's required turns out to be approximately

$$N_{\text{OPS}} = N_1/R'_1 + N_2/R'_2 \quad (2.19)$$

We thus can draw the following important observation: the number of OPS's required for the generalized factorable implementation of a GF filter defined on Λ , and of its version subsampled on a sublattice Λ' of Λ , may or may not differ, according to (2.19). In particular, if the L.D.F.L. containing Λ is also the L.D.F.L. containing Λ' , the number of OPS's will be the same in both cases. Such a result is in contrast with the case of non-factorable implementation (see Section 2.3.6), where subsampling the impulse response reduces the number of OPS's by a factor approximately equal to the subsampling ratio. Similar results are found adopting the second procedure of Observation 6.

The number of multiplications in the implementation of zero-phase 1-D filters can be reduced by exploiting the symmetry of the coefficients. However, it is important to notice that in this case only one polyphase component of $h(\mathbf{a})$ (the one centered in the origin, $h^0(\mathbf{a})$) will be zero-phase (i.e., $h^0(\mathbf{a}) = h^0(-\mathbf{a})$).

Step 4. We should now get back to the definition lattice $LAT(\mathbf{C})$ via the inverse of transformation (2.13). Each factorable coset $LAT(\mathbf{AH}) + \mathbf{r}$ is mapped into $LAT(\mathbf{CH}) + \mathbf{CA}^{-1}\mathbf{r}$ (note that $\mathbf{A}^{-1}\mathbf{r} \in Z^2$ as $\mathbf{r} \in LAT(\mathbf{A})$). In particular, points $\{kS_i\}$ on the i -th axis are mapped into points $\{k\mathbf{T}_i\}$, where \mathbf{T}_i is the i -th column of \mathbf{CH} . Hence, the r -th factorable filtering of Step 3 becomes the cascade of two generalized 1-D filterings (by the r_i -th polyphase component of $p_1(n)$ and $p_2(n)$ along the directions of \mathbf{T}_1 and \mathbf{T}_2 respectively) of signal $x(\mathbf{a})$, displaced by vector $\mathbf{CA}^{-1}\mathbf{r}$.

2.2 Generalized Factorable Filters

Let $\Lambda = LAT(\mathbf{C})$ be a M -dimensional lattice. Consider the set of points of Λ aligned along a given direction:

$$\mathcal{L}_{\mathbf{v}} = \{n\mathbf{v}, n \in Z\} \quad (2.20)$$

where $\mathbf{v} = \mathbf{C}\mathbf{n}$ with n_1 and n_2 coprime (so that $\mathcal{L}_{\mathbf{v}}$ actually spans all the points of Λ along line $a\mathbf{v}, a \in R$). A filter $h(\mathbf{a})$ such that $h(\mathbf{a}) \neq 0$ only for $\mathbf{a} \in \mathcal{L}_{\mathbf{v}}$ will be called a *generalized 1-D filter on \mathbf{v}* . Let N be the number of non-null elements of $h(\mathbf{a})$ (assume for simplicity's sake that between two non-null samples of $h(\mathbf{a})$ there is always a non-null sample). N will be called the *generalized length* of $h(\mathbf{a})$. In general, N OPS's are required to implement $h(\mathbf{a})$.

Suppose now Λ is factorable (without loss of generality, we can assume $\Lambda = Z^M$). Then $h(\mathbf{n})$ is said to be factorable [26] if it is the cascade of M 1-D filters: $h(\mathbf{n}) = \prod_{i=1}^M h_i(n_i)$. We can extend such a notion exploiting the idea of generalized 1-D filters: given a basis \mathbf{C} of Λ , we will say that $h(\mathbf{a})$ is *generalized factorable (GF) on \mathbf{C}* if $h(\mathbf{a}) = \prod_{i=1}^M h_i(\mathbf{a})$, where each filter $h_i(\mathbf{a})$ is generalized 1-D on \mathbf{C}_i . Note that such a definition applies to any lattice, and not only to factorable ones.

The idea of generalized factorability allows to classify filters that, although not factorable, can be transformed, via a change of basis of the definition lattice, into factorable filters. Hence, they can be implemented with a number of OPS's that grows linearly with the sum of the lengths of their impulse response's edges (instead that with the product of such lengths, like in the direct implementation). However, we have just seen that other filters share such a property, although they are not GF (as a matter of fact, a filter designed using the algorithm of Section 2.1 is GF only if the decimation matrix \mathbf{A} is unimodular). We are thus led to define the class of **V**-generalized factorable filters.

Let \mathbf{V} be an integral matrix, and let $\Lambda' = LAT(\mathbf{C}\mathbf{V})$ be a sublattice of Λ . A filter $h(\mathbf{a})$ defined on Λ is **V**-generalized factorable (**V**-GF) if

$$h(\mathbf{s} + \mathbf{r}) = h^r(\mathbf{s}), \mathbf{s} \in \Lambda', \mathbf{r} \in P(\Lambda', \Lambda), h^r(\mathbf{s}) \text{ generalized factorable on } \mathbf{C}\mathbf{V} \quad (2.21)$$

i.e., if its **V**-polyphase components are GF on $\mathbf{C}\mathbf{V}$.

A **V**-GF filter is also **VD**-GF for any integral diagonal matrix \mathbf{D} . Moreover, for any FIR filter $h(\mathbf{a})$ it is always possible to find a matrix \mathbf{V} such that $h(\mathbf{a})$ is **V**-GF. To prove this, one just needs to choose a matrix \mathbf{V} with sufficiently large $|\det(\mathbf{V})|$, so that the support of $h(\mathbf{a})$ is contained within some elementary cell of $\Lambda' = LAT(\mathbf{C}\mathbf{V})$. Hence, it makes sense to define the *factorability basis* of a filter $h(\mathbf{a})$ as the matrix \mathbf{V} with the smallest value of $|\det(\mathbf{V})|$, such that $h(\mathbf{a})$ is **V**-GF.

It should be clear now that filters designed using the algorithm of Chen and Vaidyanathan have factorability basis $\mathbf{C}\mathbf{H}$ (according to the notation of Section 2.1.1). In particular, the procedure of Section 2.1 represents the only known algorithm to design **V**-GF filters¹.

2.3 Some properties of GF filters

2.3.1 Preservation of the Nyquist property [28]

2.3.2 Frequency response constraints

If the filter to be designed is part of a sampling structure converter, it is useful to impose some constraints on its frequency response. For example, if the filter is expected to cancel the undesired spectral repetitions occurring when up-sampling from lattice $\Lambda_1 = LAT(\mathbf{C}\mathbf{H})$ to lattice $\Lambda = LAT(\mathbf{C})$ ($\Lambda_1 \subset \Lambda$), an important requirement is that $H(\mathbf{f})$ be vanishing for $\mathbf{f} \in \Lambda_1^*/\Lambda^*$ [29],[14], so that the aliasing due to flat brightness areas is removed. It is shown in the following how such a constraint on $H(\mathbf{f})$ can be converted into constraints on the two 1-D filters $q_1(n)$ and $q_2(n)$.

From (2.11) one has that a sufficient condition for $H(\mathbf{f})$ to be null for some $\mathbf{f} = \bar{\mathbf{f}}$ is

$$\bar{H}(\mathbf{A}^{-T}(\mathbf{C}^T\bar{\mathbf{f}} + \mathbf{r})) = 0, \mathbf{r} \in Z^2 \quad (2.22)$$

¹We will adopt a certain sloppiness in the language, and call "generalized factorable" any "**V**-generalized factorable" filter. The "real" GF filters are actually **V**-GF with unimodular \mathbf{V} . And the "real" factorable filter are GF with unimodular \mathbf{C} and $\mathbf{V} = \mathbf{C}^{-1}$. In plus, since the filters of Section 2.1 are the only **V**-GF used in the practice, we will generally address them as GF.

In our case of interest, $H(\mathbf{f})$ should vanish for

$$\mathbf{f} \in \Lambda_1^*/\Lambda^* \quad (2.23)$$

i.e., for

$$\mathbf{f} \in \{(\mathbf{C}\mathbf{H})^{-T}\mathbf{n}, \mathbf{n} \in Z^2/LAT(\mathbf{H}^T)\} \quad (2.24)$$

Substituting (2.24) for $\bar{\mathbf{f}}$ in (2.23), one gets the corresponding constraint on $\bar{H}(\mathbf{f})$:

$$\bar{H}(\mathbf{A}^{-T}(\mathbf{H}^{-T}\mathbf{n} + \mathbf{r})), \mathbf{n} \in Z^2/LAT(\mathbf{H}^T), \mathbf{r} \in Z^2 \quad (2.25)$$

i.e., $\bar{H}(\mathbf{f})$ should vanish for \mathbf{f} belonging to set

$$\begin{aligned} & (LAT(\mathbf{A}\mathbf{H})^{-T} + LAT(\mathbf{A}^{-T})) / (LAT(\mathbf{A}^{-T}) + LAT(\mathbf{A}^{-T})) \\ & = LAT((\mathbf{A}\mathbf{H})^{-T}) / LAT(\mathbf{A}^{-T}) \end{aligned} \quad (2.26)$$

Since $\bar{H}(\mathbf{f})$ is periodic on Z^2 , condition (2.26) is equivalent to

$$\bar{H}(\mathbf{f}) = 0, \mathbf{f} \in \mathcal{Z} \stackrel{\text{def}}{=} P(Z^2, LAT((\mathbf{A}\mathbf{H})^{-T}) / LAT(\mathbf{A}^{-T})) \quad (2.27)$$

To have $\bar{H}(\mathbf{f})$ vanishing in the $(|\det(\mathbf{A})|(|\det(\mathbf{H})| - 1))$ points of \mathcal{Z} , one should set $Q_1(f_1) = 0$ and/or $Q_2(f_2) = 0$ for $(f_1, f_2)^T \in \mathcal{Z}$. We will call such points the *nulling frequencies* for the 1-D filters. It is easily seen that, given set \mathcal{Z} , there exist several combinations of nulling frequencies for $Q_1(f)$ and $Q_2(f)$. For example, for each $\mathbf{f}^i = (f_1^i, f_2^i)^T \in \mathcal{Z}$, one could set

$$Q_j(f_j^i) = 0 \text{ if } f_j^i > f_{p_j}, j = 1, 2 \quad (2.28)$$

Note that we do not want to set to zero $H(\mathbf{f})$ in “useful” frequencies, i.e., belonging to the pass-band region, as would happen if we forgot the condition in (2.28). Nevertheless, following criterion (2.28), $H(\mathbf{f})$ may be forced to zero also for some frequencies in $LAT(\mathbf{A}^{-T})$, which is not required by (2.27). As a matter of fact, \mathcal{Z}_1 and \mathcal{Z}_2 (the sets of nulling frequencies for $Q_1(f)$ and $Q_2(f)$) obtained from (2.28) are not the ones with minimum cardinality, among those satisfying the nulling constraint (2.27). Such a characteristic is important, because, as well known, adding constraints to the frequency response of 1-D filters typically increases the minimum filter length required to achieve desired specifics. We are thus led to seek for sets \mathcal{Z}_1 and \mathcal{Z}_2 with smaller cardinality. To this purpose, one can exploit the following observation: if \mathcal{Z} contains two or more points $\{\mathbf{f}^1, \mathbf{f}^2, \dots\}$ with the same component $f_j^1 = f_j^2 = \dots \stackrel{\text{def}}{=} \bar{f}_j$, then the nulling condition is satisfied for all of them simply by setting $Q_j(\bar{f}_j) = 0$.

The previous argument suggests the following procedure to find “good” sets \mathcal{Z}_1 and \mathcal{Z}_2 for a given set \mathcal{Z} .

1. For each point $(f_1^i, f_2^i)^T$ of \mathcal{Z} such that $f_1^i < f_{p_1}$ or $f_2^i < f_{p_2}$, set $Q_2(f_2^i) = 0$ or $Q_1(f_1^i) = 0$ respectively. Take these points out of \mathcal{Z} , and call $\tilde{\mathcal{Z}}$ the set of the remaining points.
2. Determine all the clusters $\{C_1^i\}$ and $\{C_2^i\}$ of points of $\tilde{\mathcal{Z}}$ having common component f_1^i or f_2^i respectively. In order to find such cluster of points, one can look for the L.D.F.L. containing $LAT((\mathbf{A}\mathbf{H})^{-T})$, determine (trivially) the points of it within a rectangular elementary cell of $LAT(\mathbf{A}^{-T})$, and for each row (or each column) of the resulting set determine which points belong to $LAT((\mathbf{A}\mathbf{H})^{-T})$.
3. Find the “minimum cost” covering of $\tilde{\mathcal{Z}}$ by elements of $\{C_1^i\}$ and $\{C_2^i\}$, i.e., the set $C_1^{i_1} \cup \dots \cup C_1^{i_r} \cup C_2^{l_1} \cup C_2^{l_s}$ with minimum cardinality covering $\tilde{\mathcal{Z}}$.
4. Set $Q_1(f) = 0$ for $f \in \{f_1^{i_1}, f_1^{i_2}, \dots, f_1^{i_r}\}$ and $Q_2(f) = 0$ for $f \in \{f_2^{l_1}, f_2^{l_2}, \dots, f_2^{l_s}\}$

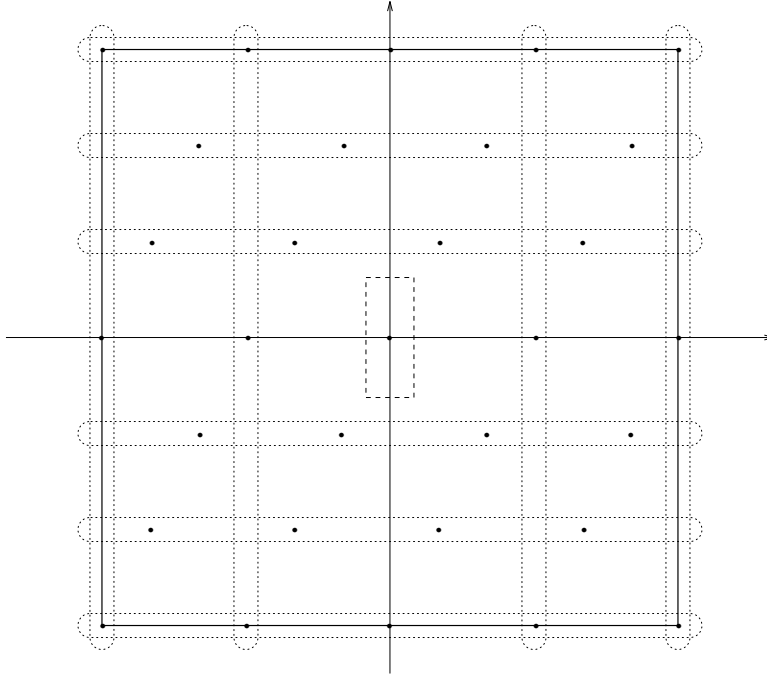


Figure 2.1: Example of nulling constraints, relative to the up-sampling from lattice $LAT(\mathbf{A}\mathbf{H})$ to lattice $LAT(\mathbf{A}) = Z^2$ (see text). The dots correspond to lattice $LAT((\mathbf{A}\mathbf{H})^{-T})$, the region contoured by solid line to the elementary cell $\mathcal{R}(0.5, 0.5)$ of Z^2 , the region contoured by dashed line to the pass-band region of $H(\mathbf{f})$, and the regions contoured by dotted lines to the clusters of points corresponding to the nulling frequencies of the two 1-D filters.

Note that, in general, there are more than one minimum cost covering of $\tilde{\mathcal{Z}}$ by clusters of $\{C_1^i\}$ and $\{C_2^i\}$. In order to design 1-D filters with frequency response constrained to zero in the chosen frequencies, one can use, for example, a technique based on linear programming [30].

As an example, consider the following case: $\mathbf{A}^{-T} = \mathbf{I}$, $(\mathbf{A}\mathbf{H})^{-T} = \begin{pmatrix} 1/4 & 1/12 \\ 0 & 1/6 \end{pmatrix}$, $f_{p_1} = 1/24$, $f_{p_2} = 1/8$. In Fig. 2.1 it is represented lattice $LAT((\mathbf{A}\mathbf{H})^{-T})$, together with the elementary cell $\mathcal{R}(1/2, 1/2)$ of $LAT(\mathbf{A}^{-T})$ (continuous line) and the pass-band region of $H(\mathbf{f})$ (dashed line). Set \mathcal{Z} corresponds with the set of points of $LAT((\mathbf{A}\mathbf{H})^{-T})$ within $\mathcal{R}(1/2, 1/2)$, excluding the origin. A minimum cost covering of \mathcal{Z} is represented by the clusters of points within the regions contoured by dotted lines. Filter $Q_1(f)$ (corresponding to the horizontal axis) is forced to zero for $f \in \{1/4, 1/2\}$, while filter $Q_2(f)$ is forced to zero for $f \in \{1/6, 1/3, 1/2\}$.

2.3.3 2-D step response

An important characteristic of filters to be implemented in video applications, is the behaviour in case of sharp brightness transitions. The “ringing” consequent to oscillatory response of the filters in such situations is visually quite noticeable [31].

In the case of 1-D filters, the response to an unitary step characterizes the filter behaviour in such critical cases. For 2-D filters, the responses of the filter to 2-D unitary steps along two or more directions, as well as to other “transition” functions, are usually considered. For example, in [32] a technique to put linear constraints in the filter design algorithm, in order to minimize the maximum amount of ripples in the vertical, horizontal and diagonal step responses, as well as in the “quadrantal step” response, is described.

GF filters are completely characterized by the two 1-D filters $q_1(n)$ and $q_2(n)$ of (2.6), together with the sampling matrix \mathbf{A} . It seems therefore of interest to examine the relationships between the step response characteristics of $q_1(n)$ and $q_2(n)$ and that of the resulting 2-D filter.

We show in the following that for two suitable 2-D steps, the output of filter $h(\mathbf{a})$ is characterized by the step responses of the decimated versions of $q_1(n)$ and $q_2(n)$. To this purpose, let $\mathbf{C} = (\mathbf{c}_1|\mathbf{c}_2)$ be a basis of the filter definition lattice, and consider function

$$S_{c_2}(k) = \sum_{n_1=-\infty}^k \sum_{n_2=-\infty}^{\infty} h(n_1\mathbf{c}_1 + n_2\mathbf{c}_2) \quad (2.29)$$

$S_{c_2}(k)$ represents the response of the filter to a 2-D step oriented along \mathbf{c}_2 , “read” along \mathbf{c}_1 . This is the best characterization of the step response, because $S_{c_2}(k)$ actually “spans” all the values of the output of the filter relative to the 2-D step. In particular, we are interested in the position of the ripples, and in the amount of the difference between each overshooting and its succeeding undershooting. Such parameters, determined by $S_{c_2}(k)$, are expected to represent a good measure of the “annoyance” of the ringing. We will show in the following how to choose orientations for the 2-D step so that the $S_{c_2}(k)$ can be related to the step responses of two decimated version of the two 1-D filters.

We can get some insight into $S_{c_2}(k)$ by considering together (2.7), (2.9) and (2.29):

$$\begin{aligned} S_{c_2}(k) &= |\det(\mathbf{A})| \sum_{n_1=-\infty}^k \sum_{n_2=-\infty}^{\infty} \bar{h}(n_1\mathbf{a}_1 + n_2\mathbf{a}_2) \\ &= |\det(\mathbf{A})| \sum_{n_1=-\infty}^k \sum_{n_2=-\infty}^{\infty} q_1(n_1A_{1,1} + n_2A_{1,2}) q_2(n_1A_{2,1} + n_2A_{2,2}) \end{aligned} \quad (2.30)$$

where $(\mathbf{a}_1|\mathbf{a}_2) = \mathbf{A}$. It is apparent that if

$$A_{1,2} = A_{2,1} = 0 \quad (2.31)$$

then $S_{c_2}(k)$ coincides with the step response of filter $q_1(nA_{1,1})$, times constant ($|\det(\mathbf{A})| \sum_{n=-\infty}^{\infty} q_2(nA_{2,2})$). One can show that, for ideal ² low-pass $q_2(n)$, the last term is equal to $|\det(\mathbf{A})|/|A_{2,2}| = |A_{1,1}|$ (as the stop-band frequency of $q_2(n)$, in this case, must be smaller than $0.5/A_{2,2}$).

Note that condition (2.31) implies that \mathbf{A} be diagonal, i.e., that the decimation lattice be factorable. In the general case, it is convenient considering a basis $\bar{\mathbf{A}} = \mathbf{A}\bar{\mathbf{U}}$ of the decimation lattice, such that $\bar{\mathbf{A}} = (\bar{\mathbf{a}}_1|\bar{\mathbf{a}}_2)$ is in lower Hermite normal form (then $\bar{A}_{1,2} = 0$). Let $\bar{\mathbf{C}} = (\bar{\mathbf{c}}_1|\bar{\mathbf{c}}_2) = \mathbf{C}\bar{\mathbf{U}}$. Then

$$S_{\bar{c}_2}(k) = |\det(\mathbf{A})| \sum_{n_1=-\infty}^k \left(q_1(n_1\bar{A}_{1,1}) \sum_{n_2=-\infty}^{\infty} q_2(n_1\bar{A}_{2,1} + n_2\bar{A}_{2,2}) \right) \quad (2.32)$$

Consider a poliphase decomposition of $q_2(n)$:

$$q_2(n) = q_2^{s(n)}(\lfloor n/\bar{A}_{2,2} \rfloor) \quad (2.33)$$

where

$$s(n) = n \bmod \bar{A}_{2,2} \quad (2.34)$$

and

$$q_2^s(n) = q_2(\bar{A}_{2,2}n + s) \quad (2.35)$$

²Actually, it is not necessary that $q_2(n)$ be ideal. A milder condition is $Q_2(0) = 1$ and $Q_2(l/(2A_{2,2})) = 0$ for $1 < l < A_{2,2}$.

Then, calling

$$Q_2^r = \sum_{n=-\infty}^{\infty} q_2^r(n) \quad (2.36)$$

and

$$r(n) = (n\bar{A}_{2,1}) \bmod \bar{A}_{2,2} \quad (2.37)$$

we can rewrite (2.32) as

$$S_{\bar{c}_2}(k) = |\det(\mathbf{A})| \sum_{n=-\infty}^k q_1(n\bar{A}_{1,1}) Q_2^{r(n)} \quad (2.38)$$

Equation (2.38) shows that the output of filter $h(\mathbf{a})$ to a 2-D step oriented along \bar{c}_2 , “read” along points $k\bar{c}_1$, coincides with the step response of the 1-D filter with impulse response $q_1(n\bar{A}_{1,1}) Q_2^{r(n)}$. If function Q_2^r is constant with respect to r , we have that the 2-D step response coincides with the step response of a decimated version of $q_1(n)$, times a multiplicative constant depending on $q_2(n)$. The following equality holds:

$$\bar{A}_{2,2} Q_2^r = Q_2(0) + 2 \sum_{k=1}^{[(\bar{A}_{2,2}-1)/2]} Q_2\left(\frac{k}{\bar{A}_{2,2}}\right) \cos\left(2\pi \frac{kr}{\bar{A}_{2,2}}\right) + \begin{cases} Q_2(0.5) & , \text{ even } \bar{A}_{2,2} \\ 0 & , \text{ odd } \bar{A}_{2,2} \end{cases} \quad (2.39)$$

hence, a sufficient condition to have constant Q_2^r is

$$Q_2(k/A_{2,2}) = 0 \text{ for } k > 0 \quad (2.40)$$

If such a case is verified, the considered 2-D step response is determined by $q_1(n)$ only. Note that, as long as the stop-band frequency of $Q_1(f)$ is smaller than $0.5/\bar{A}_{1,1}$, it is reasonable to assume that the step response behaviour of filter $q_1(n)$ does not differ “too much” from the one corresponding to its decimated version $\bar{A}_{1,1} q_1(\bar{A}_{1,1}n)$. For example, in the case of an ideal filter $h_{\text{id}}(n)$ with pass-band frequency equal to $0.5/M$ for some even integer M , the difference $\bar{D}(k)$ between the k -th overshooting and its succeeding undershooting in the step response of $h_{\text{id}}(2n)$ is between 79 and 84 per cent of $D(k)$, the correspondent value for $h_{\text{id}}(n)$ (in Appendix C such a result is proved, together with the dependance of $\bar{D}(k)/D(k)$ on k and M).

Completely similar considerations hold for the filter response to a 2-D step oriented along \hat{c}_1 , where $(\hat{c}_1|\hat{c}_2) = \mathbf{C}\hat{\mathbf{U}}$ and $\hat{\mathbf{U}}$ is such that $\mathbf{A}\hat{\mathbf{U}}$ is in upper Hermite normal form.

2.3.4 Symmetries

Impulse responses of M-D FIR filters defined on lattices often enjoy symmetries, which can be exploited in order to reduce the computational weight (in terms of number of OPS's) [33]. The kind of symmetry we will consider here is the one derived by a *spatially complete congruent* mapping (i.e., $\Lambda \rightarrow \Lambda$ bijective) [33]. In other words, given filter $h(\mathbf{C}\mathbf{n})$, we are looking for an integral unimodular matrix \mathbf{Q} such that

$$h(\mathbf{C}\mathbf{n}) = h(\mathbf{C}\mathbf{Q}\mathbf{n}), \mathbf{n} \in Z^2 \quad (2.41)$$

It is useful, for the arguments of this section, defining the following integral unimodular matrices:

$$\mathbf{Q}_1 = \mathbf{I} = \begin{pmatrix} 1 & 0 \\ 0 & 1 \end{pmatrix}, \mathbf{Q}_2 = \begin{pmatrix} 0 & 1 \\ 1 & 0 \end{pmatrix}, \mathbf{Q}_3(b) = \begin{pmatrix} 1 & b \\ 0 & -1 \end{pmatrix}, \mathbf{Q}_4(c) = \begin{pmatrix} 1 & 0 \\ c & -1 \end{pmatrix} \quad (2.42)$$

where b and c are integer. The matrices of (2.42) characterize the set \mathcal{Q} of 2×2 integral matrices that coincide with their own inverse:

$$\mathcal{Q} = \{\pm\mathbf{Q}_1, \pm\mathbf{Q}_2, \pm\mathbf{Q}_3(b), \pm\mathbf{Q}_4(c), b, c \in Z\} \quad (2.43)$$

If the 1-D filters $q_1(n)$ and $q_2(n)$ are zero-phase (as we have assumed so far), then filter $\bar{h}(\mathbf{n})$ as in (2.7) enjoys property

$$\bar{h}(\mathbf{n}) = \bar{h}(\mathbf{Q}\mathbf{n}) , \quad \mathbf{Q} \in \{\pm\mathbf{Q}_1, \pm\mathbf{Q}_3(0)\} \quad (2.44)$$

Its sampled version $\bar{h}(\mathbf{A}\mathbf{n})$ (see (2.9)) enjoys property (from (2.44))

$$\bar{h}(\mathbf{A}\mathbf{n}) = \bar{h}(\mathbf{Q}\mathbf{A}\mathbf{n}) , \quad \mathbf{Q} \in \{\pm\mathbf{Q}_1, \pm\mathbf{Q}_3(0)\} , \quad \mathbf{Q}\mathbf{A}\mathbf{n} \in LAT(\mathbf{A}) \quad (2.45)$$

In order for the mapping specified by \mathbf{Q} to be complete, the last condition of (2.45) should hold for each $\mathbf{n} \in Z^2$. This is equivalent to (remember that \mathbf{Q} is unimodular)

$$LAT(\mathbf{Q}\mathbf{A}) = LAT(\mathbf{A}) \quad (2.46)$$

i.e., to

$$\mathbf{A}^{-1}\mathbf{Q}\mathbf{A} \in Z_2 \quad (2.47)$$

This condition is trivially satisfied if \mathbf{A} is unimodular. Assume now $|\det(\mathbf{A})| > 1$. Note that, since $\det(\mathbf{A}^{-1}\mathbf{Q}\mathbf{A}) = \pm 1$, condition (2.47) is equivalent to

$$(\mathbf{A}^{-1}\mathbf{Q}\mathbf{A})^{-1} = \mathbf{A}^{-1}\mathbf{Q}^{-1}\mathbf{A} = \mathbf{A}^{-1}\mathbf{Q}\mathbf{A} \in Z_2 \quad (2.48)$$

and therefore $\mathbf{A}^{-1}\mathbf{Q}\mathbf{A} = \mathbf{Q}_j$ for some $\mathbf{Q}_j \in \mathcal{Q}$. We can rewrite this last identity as

$$\mathbf{Q}\mathbf{A} = \mathbf{A}\mathbf{Q}_j \quad (2.49)$$

Assume \mathbf{A} is in upper Hermite normal form. If this was not the case, it is always possible to change basis in Λ so that such an hypothesis is met. We should now determine when (2.47) is satisfied for $\mathbf{Q} \in \{\pm\mathbf{Q}_1, \pm\mathbf{Q}_3(0)\}$. Cases $\mathbf{Q} = \pm\mathbf{Q}_1$ are trivial. In particular, $-\mathbf{Q}_1\mathbf{A} = -\mathbf{A}\mathbf{Q}_1$, i.e., employing zero-phase 1-D filters, the resulting 2-D filter is zero-phase. This property was already noted in [28].

It remains to check case $\mathbf{Q} = \pm\mathbf{Q}_3(0)$, which can be verified by direct inspection. Condition (2.47) is never satisfied for $\mathbf{Q} = \pm\mathbf{Q}_3(0)$, $\mathbf{Q}_j = \mathbf{Q}_2$. Case $\mathbf{Q}_j = \mathbf{Q}_3(0) = \mathbf{Q}_4(0)$ satisfies (2.47) only if \mathbf{A} is diagonal, but, according to Observation 5 of Section 2.1, this implies $\mathbf{A} = \mathbf{I}$, and we are back to the case of unimodular \mathbf{A} . The only other case for which condition (2.47) is satisfied when $\mathbf{Q} = \pm\mathbf{Q}_3(0)$, is for $\mathbf{Q}_j = \pm\mathbf{Q}_3(1)$ if $A_{1,1} = 2A_{1,2}$.

Let us summarize the results of this section. Assume the 1-D filters $q_1(n)$ and $q_2(n)$ are zero-phase. Then $h(\mathbf{C}\mathbf{n}) = h(-\mathbf{C}\mathbf{n})$. Moreover, if the decimation matrix \mathbf{A} is unimodular, then

$$h(\mathbf{C}\mathbf{n}) = h(\pm\mathbf{C}\mathbf{Q}_3(0)\mathbf{n}) \quad (2.50)$$

Such a relation can be regarded to as a quadrantal-like symmetry.

If \mathbf{A} is not unimodular, let $\bar{\mathbf{A}}$ be the upper Hermite normal form matrix associate to \mathbf{A} . Then relation (2.50) is verified if (and only if) $\bar{A}_{1,1} = 2\bar{A}_{1,2}$.

2.3.5 Optimality in the least squares sense

A GF filter designed by truncating the impulse responses of 1-D ideal filters of (2.6) provides, as a matter of fact, the optimal least squares approximation (among the FIR filters with support equal to (2.12)) to the ideal transfer function $H(\mathbf{f})$ in (2.8). This is immediately derived from [28], where the explicit relations between ideal $h(\mathbf{C}\mathbf{n})$ and ideal $\{q_i(n)\}$ are computed.

2.3.6 Minimax parameters

It can be interesting looking for relations among overall (conventional) filter length, pass-band and stop-band ripples, and some measure of the “size” of the transition region, that hold in GF filters designed starting from optimal minimax 1-D filters.

Adopting the notation of Section 2.1, from Observation 4 in the same section it is immediately seen that

$$\mathbf{F}_p \stackrel{\text{def}}{=} \text{diag}(f_{p_1}, f_{p_2}) = \mathbf{A}^{-T} \mathbf{C}^T \mathbf{P}_p \quad (2.51)$$

$$\mathbf{F}_s \stackrel{\text{def}}{=} \text{diag}(f_{s_1}, f_{s_2}) = \mathbf{A}^{-T} \mathbf{C}^T \mathbf{P}_s \quad (2.52)$$

Noting that $|\det(\mathbf{F}_s - \mathbf{F}_p)| = |\det(\mathbf{A}^{-T} \mathbf{C}^T (\mathbf{P}_s - \mathbf{P}_p))| = 2B_{t_1} B_{t_2}$, where $B_{t_i} = f_{s_i} - f_{p_i}$, we have that, for given pass-band and stop-band parallelograms specifying the support of $H(\mathbf{f})$, the product of the transition bandwidths of filters $q_1(n)$ and $q_2(n)$ (and therefore term $1/N_1 N_2$, for given pass-band and stop-band ripples δ_{p_i} and δ_{s_i} of the two 1-D filters, see (1.2)) is proportional to $|\det(\mathbf{C})|/|\det(\mathbf{A})|$. The conventional length N_c of filter $h(\mathbf{a})$ is approximately equal to $N_1 N_2/|\det(\mathbf{A})|$; we thus maintain that, for given pass-band and stop-band ripples of $Q_1(f)$ and $Q_2(f)$, N_c can be considered approximately inversely proportional to $|\det(\mathbf{C})|$ and independent of \mathbf{A} . Similarly, for given values of $\det(\mathbf{C})/\det(\mathbf{A})$, the conventional length N_c is approximately inversely proportional to $\det(\mathbf{P}_s - \mathbf{P}_p)$ (which represents the area \mathcal{A} of the “corner region” depicted in Fig. 2.2):

$$\mathcal{A} \cdot N_c \simeq \text{constant} \quad (2.53)$$

It is apparent the resemblance between such a result and the relation between transition bandwidth, ripples and length of minimax 1-D filters (1.2). A more careful exam, though, shows that the situation is actually quite tricky. As a matter of fact, relation (2.53) holds for fixed ripples $\delta_{p_i}, \delta_{s_i}$ of the two 1-D filters. The relation between $\{\delta_{p_i}, \delta_{s_i}\}$ and $\{\delta_p, \delta_s\}$ (the ripples of the resulting 2-D filter), is obtained combining together inequalities (B.13),(B.14) and (B.16),(B.17):

$$\delta_p \leq \delta_{p_1} + \delta_{p_2} + (|\det(\mathbf{A}) - 1|) \max\{\delta_{s_1}, \delta_{s_2}\} \quad (2.54)$$

$$\delta_s \leq |\det(\mathbf{A})| \max\{\delta_{s_1}, \delta_{s_2}\} \quad (2.55)$$

We can obtain a simple worst-case relation between $\delta_p \delta_s$ and N_c (for fixed area \mathcal{A}) if $\delta_{p_1} = \delta_{p_2} = \delta_{s_1} = \delta_{s_2} \stackrel{\text{def}}{=} \delta$. In such a case, it is

$$\delta_p \delta_s \leq |\det(\mathbf{A})| (|\det(\mathbf{A}) + 1|) \delta^2 \quad (2.56)$$

As a matter of fact, inequality (2.56) turns out not to be of much usefulness in practice. The derived upper bound is very pessimistic, and experimental tests show that one can actually reach much smaller values for $\delta_p \delta_s$. On the other side, the lack of a theoretical expression for the lower bound for $\delta_p \delta_s$ in the 2-D case (see Appendix B) makes it difficult to predict the actual characteristics of the resulting filter.

As an operative rule of thumb, we will accept the following simple approximation for GF filters: term $\delta_p \delta_s$ decreases as the product $\mathcal{A} \cdot N_c$ increases. Due to the unpredictable effect of the contributions of the frequency response oscillations of the two 1-D filters, our statement may not hold true in some instances. A general theory capable of predicting such a behaviour is beyond the scope of the present work. Nonetheless, experimental tests show that these situations are not frequent in practice, and we will keep to our assumption as a guideline criterion for the procedure of Section 3. Clearly, our hypothesis is more likely to hold true for small values of $|\det(\mathbf{A})|$. The higher the number of overlapping spectral repetitions, the more unpredictable the behaviour of the frequency response. This is one of the reasons why, in the GF filter design algorithm, one seeks for decimation matrices \mathbf{A} with the smallest value of $|\det(\mathbf{A})|$ (another reason being that – as already noted – large values of $|\det(\mathbf{A})|$ typically induce the pass-band and transition band of filters $q_i(n)$ to be narrow, with consequent increase of the design burden).

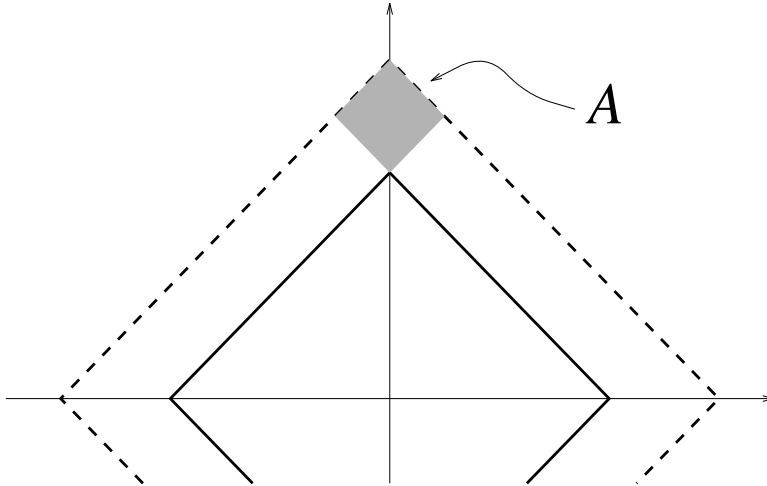


Figure 2.2: Example of “corner region” for a diamond-shaped spectral mask. Solid line: pass-band curve. Dashed line: stop-band curve.

In closing this section, it is interesting to notice that, starting from 1-D optimal minimax filters, one does not obtain the best minimax approximation (in the class of GF filters), to the ideal frequency response of (2.8), as it is easily proved. The determination of the constraints to put on the 1-D filters in order to get the optimal minimax solution remains an open issue.

Chapter 3

2-D IFIR Filters

IFIR filters can be profitable in the 2-D case as well as in the 1-D case. The computational weight, in terms of number of OPS's, can be effectively reduced with respect to conventional filters, depending on the characteristics of the ideal frequency response to approximate and on the definition lattice. Although precise relationships among filter parameters are not available in general for 2-D filters, in the case of GF filters one can exploit the indications of Section 2.3.6 to characterize the filter behaviour, and to devise efficient schemes for IFIR structures.

In the evaluation of the achievable computational weight reduction, it is important to consider how the filters are implemented. In particular, the use of the generalized factorable implementation determines dramatically the improvements attainable via an IFIR scheme. A simple example will make such an argument clear.

Consider a factorable filter $d(\mathbf{n})$ defined on Z^2 : $d(\mathbf{n}) = d_1(n_1)d_2(n_2)$. Let N_1 and N_2 be the lengths of $d_1(n_1)$ and $d_2(n_2)$ respectively, so that $N = N_1N_2$ is the length of $d(\mathbf{n})$. Implementing $d(\mathbf{n})$ without taking into account the factorability requires N OPS's (exploiting symmetries in $d(\mathbf{n})$ can reduce the number of multiplications by some constant factor). If we adopt the factorable implementation, only $N_1 + N_2$ OPS's are required (again, we neglect symmetries in the impulse responses). Assume now to use a 1-D IFIR structure for both $d_1(n)$ and $d_2(n)$. For instance, we may have

$$D_i(z) = H_i(z^2)G_i(z), \quad i = 1, 2 \quad (3.1)$$

Let N_{h_i} and N_{g_i} be the lengths of filters $h_i(n)$ (without null samples interleaved!) and $g_i(n)$ respectively, and suppose $N_{h_i} + N_{g_i} = N_i/2$ (for details about actual performances of 1-D IFIR filters, see [1],[6]). It is straightforward that, using the factorable implementation of the 2-D filter, now only $(N_1 + N_2)/2$ OPS's are required. On the other side, if the filter is implemented in a non-factorable fashion, one easily realizes (see Fig. 3.1) that the whole structure is equivalent to the cascade of two 2-D filters, the first of whom having non-null samples only on lattice $LAT(2 \mathbf{I})$. The number of OPS's required to implement the cascade of two filters is the sum of their conventional lengths (defined in Appendix B), i.e.

$$N^{\text{IFIR}} = N_{h_1}N_{h_2} + N_{g_1}N_{g_2} \quad (3.2)$$

If $N_{h_1} = N_{h_2} \stackrel{\text{def}}{=} N_h$ and $N_{g_1} = N_{g_2} \stackrel{\text{def}}{=} N_g$, then $N^{\text{IFIR}} = N^2/4 - 2N_hN_g$. Hence, with respect to the "direct" filter, using such an IFIR scheme with a non-factorable implementation requires less than 25% of OPS's than in the direct case. In general, if IFIR structures of the form $H(z^M)G(z)$ are used, the computational burden can be reduced approximately by a factor M in the factorable case, and by a factor M^2 in the non-factorable case.

The scheme described so far is actually the simplest IFIR structure for 2-D signals. In general, a two-stages 2-D IFIR filter defined on a lattice $LAT(\mathbf{C})$ is composed by the cascade of two filters, $h(\mathbf{a})$ and $g(\mathbf{a})$, where $h(\mathbf{a})$ has non-null coefficients only on a sublattice $LAT(\mathbf{CH})$. As it will

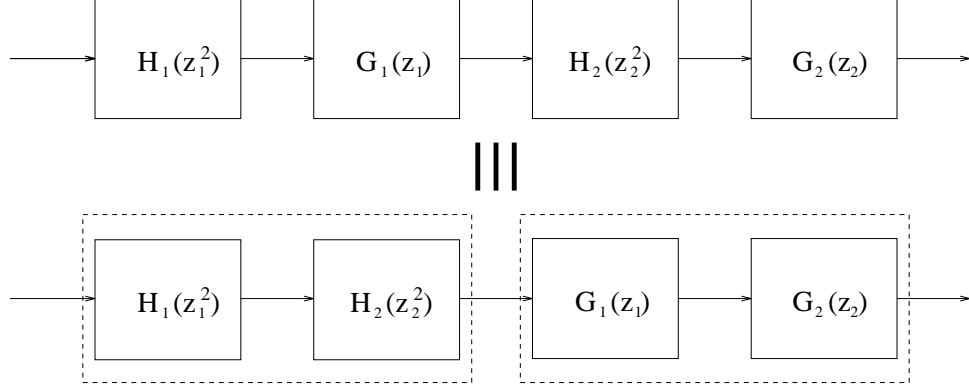


Figure 3.1: The cascade of two 1-D IFIR filters (on z_1 and z_2 respectively) is equivalent to a 2-D IFIR filter.

be shown in the following, the dependance of the overall computational weight reduction factor on term $|\det(\mathbf{H})|$ is roughly linear in the case of non-factorable implementation. The situation is less straightforward using the generalized factorable implementation, and it can be interpreted in terms of the results of Section 2.1.1.

3.1 2-D IFIR Schemes with GF Filters

Let $\Lambda = LAT(\mathbf{C})$ be the signal definition lattice, and consider a sequence $\mathcal{L} = (\Lambda_0, \Lambda_1, \dots, \Lambda_{M-1})$ of lattices such that

$$\Lambda_0 \stackrel{\text{def}}{=} \Lambda \supset \Lambda_1 = LAT(\mathbf{C}\mathbf{H}_1) \supset \dots \supset \Lambda_{M-1} = LAT(\mathbf{C}\mathbf{H}_1\mathbf{H}_2 \dots \mathbf{H}_{M-1}) \quad (3.3)$$

We then define an IFIR structure on \mathcal{L} as the cascade of M FIR filters $(h^1(\mathbf{a}), h^2(\mathbf{a}), \dots, h^{M-1}(\mathbf{a}))$ defined on Λ , such that $h^i(\mathbf{a})$ has non-null coefficients only on Λ_i . Note that $H^i(\mathbf{f})$ is periodic on Λ_i^* .

In this work, we will consider only case $M = 2$, and define $\mathbf{H} = \mathbf{H}_1$. Note that in any elementary cell of Λ there are $|\det(\mathbf{H})|$ spectral repetitions of $H^1(\mathbf{f})$.

Let $H_{id}(\mathbf{f})$ be the ideal frequency response to be approximated by $H^0(\mathbf{f})H^1(\mathbf{f})$. We will consider here $H_{id}(\mathbf{f})$ of the form

$$H_d(\mathbf{f}) = \begin{cases} 1 & , \mathbf{f} \in Par(\mathbf{v}_1|\mathbf{v}_2) \\ 0 & , \mathbf{f} \in \mathcal{V}/Par(\alpha\mathbf{v}_1|\alpha\mathbf{v}_2) , \alpha > 1 \end{cases} \quad (3.4)$$

where \mathcal{V} is a suitable elementary cell of Λ^* such that $Par(\alpha\mathbf{v}_1|\alpha\mathbf{v}_2) \subset \mathcal{V}$. Note that we allow for a transition region $Par(\alpha\mathbf{v}_1|\alpha\mathbf{v}_2)/Par(\mathbf{v}_1|\mathbf{v}_2)$. We also put the condition that $Par(\alpha\mathbf{v}_1|\alpha\mathbf{v}_2)$ be contained within an elementary cell of $\Lambda_1^* = LAT((\mathbf{A}\mathbf{H})^{-T})$.

Our approach to the design of $h^0(\mathbf{a})$ and $h^1(\mathbf{a})$ is the following: we design $H^1(\mathbf{f})$ (the “shaping” filter [6]) which approximates $H_{id}(\mathbf{f})$ within \mathcal{V} . We then design $H^0(\mathbf{f})$ (the “interpolator” filter) so as to cancel the $|\det(\mathbf{H})| - 1$ undesired spectral repetitions of $H^1(\mathbf{f})$ within \mathcal{V} . Following such a procedure, it is natural to choose for $H^1(\mathbf{f})$ a GF filter defined on Λ_1 , and then to up-sample it on Λ . The interpolated filter $H^0(\mathbf{f})$, however, is not bound to exhibit any particular shape. As a matter of fact, the requirements for the interpolator are:

$$\mathcal{P}_{H^0} \supset Par(\mathbf{v}_1|\mathbf{v}_2) , \mathcal{S}_{H^0} \supset \{Par(\alpha\mathbf{v}_1|\alpha\mathbf{v}_2) + \mathbf{s} , \mathbf{s} \in P(\Lambda^*, \Lambda_1^*)\} \quad (3.5)$$

where \mathcal{P}_{H^0} and \mathcal{S}_{H^0} are the pass-band and stop-band regions of $H^0(\mathbf{f})$ (as defined in Appendix B).

In our algorithm, we decided to design $H^0(\mathbf{f})$ as a GF filter, with pass-band's sides parallel to those of $Par(\mathbf{v}_1|\mathbf{v}_2)$. We do not claim that this is the “best” solution; but, as we are dealing with parallelogram-shaped pass-band regions, it seems at least a reasonable choice. In plus, our method has the advantage that it can be easily automatized. In the next section, we describe an algorithm to find the shapes of the interpolator filters that provide efficient realizations, starting from the the spectral mask $Par(\mathbf{v}_1|\mathbf{v}_2)$, the definition lattice Λ and its sublattice Λ_1 .

3.2 Design of the Interpolator

As mentioned above, we design the interpolator filter as a GF filter, with pass-band's sides parallel to those of $P(\mathbf{v}_1|\mathbf{v}_2)$, satisfying (3.5). Note that (3.5) does not constrain the frequency response of $H^0(\mathbf{f})$ in points that belong neither to the repetitions of $P(\mathbf{v}_1|\mathbf{v}_2)$ on Λ^* nor to the repetitions of $P(\alpha\mathbf{v}_1|\alpha\mathbf{v}_2)$ on Λ_1^*/Λ^* . Hence, infinite choices for $H^0(\mathbf{f})$ are available, and we should pick up the one we expect to be the “best” in terms of computational burden.

We showed in Section 2.3.6 that, in general, the minimum filter length to achieve given minimax filter parameters decreases with the corner area of the transition region. Therefore, our rule to choose the pass-band and stop-band region of the interpolator will be maximizing the corner area, while satisfying (3.5).

Following such a criterion, it is straightforward that the pass-band region of $H^0(\mathbf{f})$ should coincide with $P(\mathbf{v}_1|\mathbf{v}_2)$. On the other side, one can easily verify that several feasible candidates for the stop-band region are available in general. They are like “local maxima” of a function (the corner region area) of the stop-band region. We will show in the following how to find such local maxima; once they have been determined, we will pick up the one that requires the minimum filter length to attain the desired minimax filter parameters.

In order to describe our procedure, it is convenient looking at the “transformed” signals (see (2.9))

$$\bar{h}^0(\mathbf{A}\mathbf{n}) = h^0(\mathbf{C}\mathbf{n}), \quad \bar{h}^1(\mathbf{A}\mathbf{n}) = h^1(\mathbf{C}\mathbf{n}) \quad (3.6)$$

Now all the pass-band and stop-band regions are rectangular with sides pairwise parallel to the cartesian axes. The pass-band region $P(\mathbf{v}_1|\mathbf{v}_2)$ is transformed into $P(\mathbf{C}^{-T}\mathbf{A}^T(\mathbf{v}_1|\mathbf{v}_2)) = \mathcal{R}(\mathbf{u})$, the stop-band region $P(\alpha\mathbf{v}_1|\alpha\mathbf{v}_2)$ is transformed into $\mathcal{R}(\alpha\mathbf{u})$, the repetition lattice Λ^* is transformed into $\mathcal{L} \stackrel{\text{def}}{=} LAT(\mathbf{A}^{-T})$, and the periodicity lattice Λ_1^* becomes $\mathcal{L}_1 \stackrel{\text{def}}{=} LAT((\mathbf{A}\mathbf{H})^{-T})$. Our purpose is to find the “largest” rectangles contained in some (rectangular) elementary cell of \mathcal{L}_1 , which do not overlap any repetition of $\mathcal{R}(\alpha\mathbf{u})$ on the points of \mathcal{L}_1 . We will call such rectangles the *maximal* rectangles. More precisely, a rectangle with sides parallel to the axes is maximal if it cannot be expanded along any direction, without bumping into some repetition of itself on the points of \mathcal{L}_1 , or into some repetition of $\mathcal{R}(\alpha\mathbf{u})$ on the points of \mathcal{L}_1 . Maximal rectangles are the candidates from which the support of the stop-band of $H_0(\mathbf{f})$ will be chosen.

In the following, a simple algorithm to find all maximal rectangles, given $\mathcal{L}_1, \mathcal{L}_1, \mathbf{u}$ and α , is described. Let $\mathcal{A} = \mathcal{R}(q_1, q_2)$, where $LAT(\text{diag}(q_1, q_2))$ is the densest factorable sublattice of \mathcal{L}_1 . It is clear that the rectangular elementary cells of \mathcal{L}_1 are contained in \mathcal{A} . Let us observe since now that, in case any side of a maximal rectangle $\mathcal{R}(a_1, a_2)$ is contained within a side of \mathcal{A} (i.e., $a_1 = q_1$ (case 1) or $a_2 = q_2$ (case 2)), then the interpolator $H^0(\mathbf{f})$ can be profitably reduced to a generalized 1-D filter: we can set $\bar{H}^0(\mathbf{f}) = \bar{H}_2(f_2)$ where $\bar{H}_2(f)$ is characterized by $f_p = u_2, f_s = a_2$ (case 1), or $\bar{H}^0(\mathbf{f}) = \bar{H}_1(f_1)$ with $\bar{H}_1(f)$ characterized by $f_p = u_1, f_s = a_1$ (case 2). Note in passing that other generalized 1-D filters, oriented along different directions, can be found, satisfying (3.5). The determination of such filters, however, is beyond the scope of the present work.

The first step in the algorithm to find the maximal rectangles, is constructing an ordered set Q_1 from the points of \mathcal{L}_1 contained within rectangle¹

$$\mathcal{S} = \{\mathbf{f}, \mathbf{f} \in \mathcal{A}, f_2 \geq 0\} \quad (3.7)$$

¹A dual algorithm would interchange the role of f_1 and f_2 .

For each set of points $\{\mathbf{a}^i\}$ of $,^*_1$ contained in \mathcal{S} (except the origin), characterized by the same component a_2^i , we add point $(\min\{a_1^i\}, a_2^i)^T$ in Q_1 . Once Q_1 has been built, we construct Q_2 from Q_1 by discarding all points $(a_1^i, a_2^i)^T$ such that some other point $(a_1^j, a_2^j)^T$ exists in Q_1 with $a_1^j \leq a_1^i$ and $a_2^j \leq a_2^i$. Note that our definition is consistent (i.e. it gives rise to just one set Q_2 starting from Q_1), and that one can order the elements of Q_2 according to the ascending order of components a_2^i .

It should be not too difficult to convince oneself that the set of maximal rectangles is composed by rectangles $\mathcal{R}(\mathbf{b}^1), \mathcal{R}(\mathbf{b}^2), \dots, \mathcal{R}(\mathbf{b}^{M-1})$, with

$$b_1^i = \begin{cases} a_1^i/2 & , \mathbf{a}^i \in ,^* \\ a_1^i - \alpha u_1 & , \mathbf{a}^i \notin ,^* \end{cases} \quad (3.8)$$

and

$$b_2^i = \begin{cases} a_2^{i+1}/2 & , \mathbf{a}^{i+1} \in ,^* \\ a_2^{i+1} - \alpha u_2 & , \mathbf{a}^{i+1} \notin ,^* \end{cases} \quad (3.9)$$

A simple example should make our procedure clear. Consider the following design parameters: $\mathbf{C} = \mathbf{I}$, $\mathbf{H} = \begin{pmatrix} 2 & 1 \\ 0 & 1 \end{pmatrix}$, $\mathbf{v}_1 = (1/20, 1/40)^T$, $\mathbf{v}_2 = (-1/20, 1/40)^T$, $\alpha = 3/2$. Fig. 3.3(a) represents the repetitions of $Par((\mathbf{v}_1|\mathbf{v}_2))$ on the points of Λ_1^* . The repetitions centered on the points of Λ_1^*/Λ^* are to be cancelled by $H^0(\mathbf{f})$.

Using the algorithm of Section 2.1, one obtains the sampling matrix $\mathbf{A} = \begin{pmatrix} 2 & 1 \\ -2 & 1 \end{pmatrix}$ and the pass-band frequencies of the 1-D filters $f_{p_1} u_1 = f_{p_2} = u_2 = 1/40$. Thus $\mathbf{A}^{-T} = \begin{pmatrix} 1/4 & 1/2 \\ -1/4 & 1/2 \end{pmatrix}$ and $(\mathbf{A}\mathbf{H})^{-T} = \begin{pmatrix} -1/8 & 1/2 \\ -3/8 & 1/2 \end{pmatrix}$. The densest factorable sublattice of $,^* = LAT(\mathbf{A}^{-T})$ is $LAT\left(\begin{pmatrix} 1 & 0 \\ 0 & 1 \end{pmatrix}\right) = Z^2$, so that $\mathcal{A} = \mathcal{R}(1,1)$. We can readily find the (ordered) set Q_1 from Fig. 3.2(a):

$$Q_1 = \left\{ (1,0)^T, \left(\frac{3}{8}, \frac{1}{8}\right)^T, \left(\frac{1}{4}, \frac{1}{4}\right)^T, \left(\frac{1}{8}, \frac{3}{8}\right)^T, \left(\frac{1}{2}, \frac{1}{2}\right)^T, \left(\frac{1}{8}, \frac{5}{8}\right)^T, \left(\frac{1}{4}, \frac{3}{4}\right)^T, \left(\frac{3}{8}, \frac{7}{8}\right)^T, (0,1)^T \right\}$$

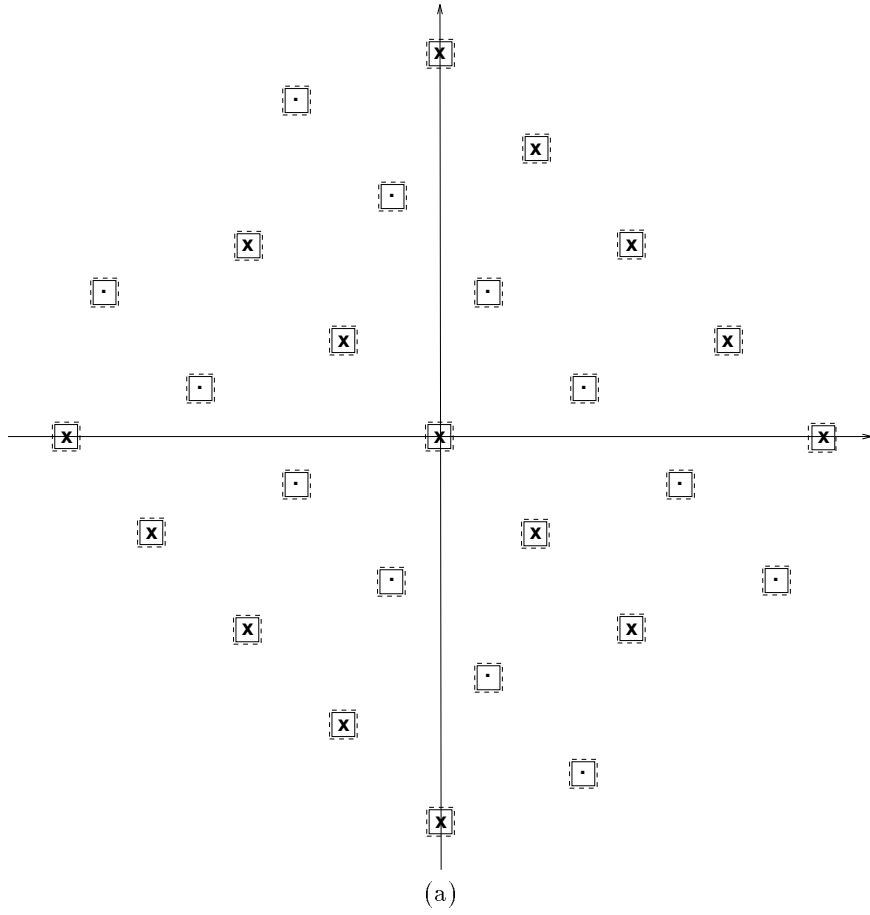
Note that one can write an automatic procedure to obtain the points of $,^*_1$ within \mathcal{A} . For example, one can determine the L.D.F.L. containing $,^*_1$, determine (trivially) the points of such lattice within \mathcal{A} , and identify those which actually belong to $,^*_1$. Next, set Q_2 is derived by Q_1 :

$$Q_2 = \left\{ (1,0)^T, \left(\frac{3}{8}, \frac{1}{8}\right)^T, \left(\frac{1}{4}, \frac{1}{4}\right)^T, \left(\frac{1}{8}, \frac{3}{8}\right)^T, (0,1)^T \right\} \quad (3.10)$$

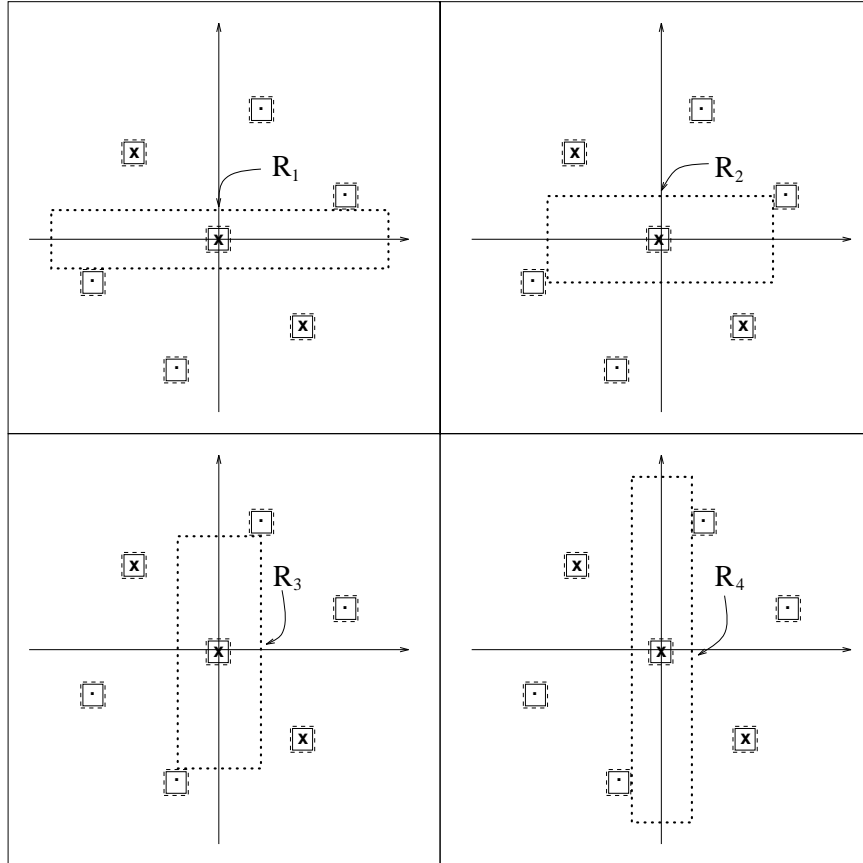
From Q_2 we build the set of maximal rectangles

$$\left\{ R_1 = \mathcal{R}\left(\frac{1}{2}, \frac{1}{8} - \frac{3}{80}\right), R_2 = \mathcal{R}\left(\frac{3}{8} - \frac{3}{80}, \frac{1}{8}\right) \right. \\ \left. R_3 = \mathcal{R}\left(\frac{1}{8}, \frac{3}{8} - \frac{3}{80}\right), R_4 = \mathcal{R}\left(\frac{1}{8} - \frac{3}{80}, \frac{1}{2}\right) \right\} \quad (3.11)$$

The maximal rectangles are depicted in Fig. 3.2(b). They correspond to the candidates for the stop-band curve of $H^0(\mathbf{f})$, represented in Fig. 3.3(b). Note that, according to our previous observation, rectangles R_1 and R_4 correspond to generalized 1-D filters. Due to the symmetry of the spectral mask of $h^1(\mathbf{f})$ and of the repetition lattice, there are two symmetric couples of such curves (namely, couple (1) and (4) and couple (2) and (3) in Fig. 3.3(b)).

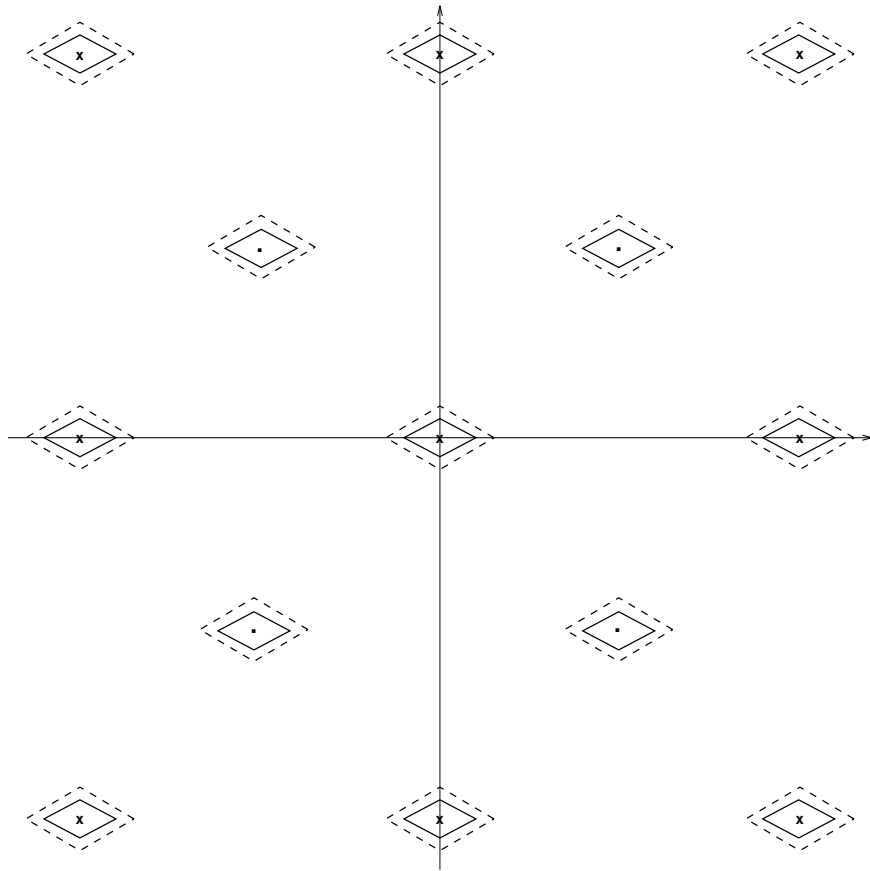


(Continued on next page)



(b)

Figure 3.2: (a) Lattice $LAT((\mathbf{A}\mathbf{H})^{-T})$ (dots), lattice $LAT(\mathbf{A}^{-T})$ (crosses), and spectral repetitions of $\bar{H}_1(\mathbf{f})$ (solid line=pass-band curve, dashed line=stop-band curve) (see text); (b) The four maximal rectangles.



(a)

(Continued on next page)

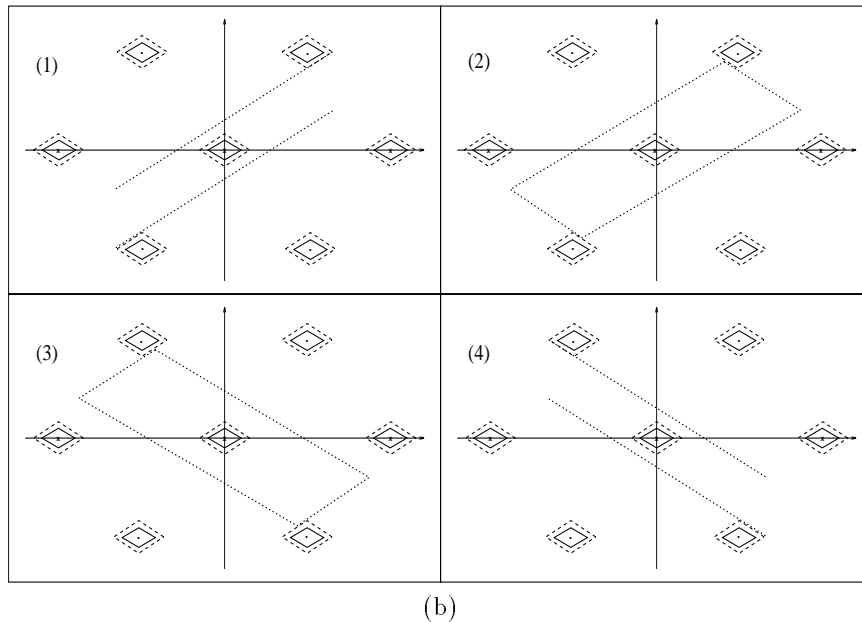


Figure 3.3: (a) Lattice $LAT((\mathbf{CH})^{-T})$ (dots), lattice $LAT(\mathbf{C}^{-T}) = Z^2$ (crosses), and spectral repetitions of $H_1(\mathbf{f})$ (solid line=pass-band curve, dashed line=stop-band curve) (see text); (b) The stop-band curves corresponding to the maximal rectangles. Only those centred in the origin are shown. Note that case (1) and (4) (corresponding to rectangles R_1 and R_4) collapse into generalized 1-D filters.

3.3 Some examples

In this section we show two examples of use of the algorithm proposed for the design of 2-D IFIR filters. For given filter specifics (in terms of spectral mask and definition lattice $\Lambda = LAT(\mathbf{C})$), we first design the shaping filter $H^1(\mathbf{f})$ on Λ . Then we consider a number of sublattices $\{\Lambda_i = LAT(\mathbf{CH}_i)\}$ of Λ , and for each of them we design the related interpolators (according to the indications of Section 3.2). The cascade of the shaping filter, with its coefficients set to zero in Λ/Λ_i , and of the different interpolators, represent the set of feasible IFIR schemes. Note that, according to Observation 6 in Section 2.1, in order to achieve the lowest possible value for $|\det(\mathbf{A})|$, it is possible in certain cases to design a new shaping filter directly on Λ_1 , instead that decimating a prototype defined on Λ . However, for the sake of simplicity we have adopted the decimation procedure in our experiments.

The performances of the IFIR filters have been evaluated in terms of pass-band and stop-band ripples (δ_p, δ_s) and of number of OPS's required for the implementation. Although we have used GF filters for both the shaping and the interpolator stages, we have considered here both the generalized factorable and the non-factorable implementation of the filters. In this way, we provide a reasonable guess of the performance attainable by IFIR schemes using filters other than GF.

In our examples, we have tested exhaustively the IFIR systems relative to all the sublattices Λ_i with index in Λ ranging from 2 to 5, correspondent to bases \mathbf{CH}_i with \mathbf{H}_i in upper Hermite normal form. Matrices $\{\mathbf{H}_i\}$ are enumerated in Tab. 3.1. For each sublattice Λ_i , the stop-band curves (corresponding to the maximal rectangles) are found. It will be seen that, depending on the shape of the desired frequency response mask, some times more than one “maximal” stop-band curves exist, while in other cases no one can be found. In this latter case, the IFIR structure relative to such a sublattice is not feasible. In some instances (like in the case of Fig. 3.3), there

$\mathbf{H}_2 = \begin{pmatrix} 2 & 0 \\ 0 & 1 \end{pmatrix}$	$\mathbf{H}_3 = \begin{pmatrix} 2 & 1 \\ 0 & 1 \end{pmatrix}$	$\mathbf{H}_4 = \begin{pmatrix} 1 & 0 \\ 0 & 2 \end{pmatrix}$	$\mathbf{H}_5 = \begin{pmatrix} 3 & 0 \\ 0 & 1 \end{pmatrix}$
$\mathbf{H}_6 = \begin{pmatrix} 3 & 1 \\ 0 & 1 \end{pmatrix}$	$\mathbf{H}_7 = \begin{pmatrix} 3 & 2 \\ 0 & 2 \end{pmatrix}$	$\mathbf{H}_8 = \begin{pmatrix} 1 & 0 \\ 0 & 3 \end{pmatrix}$	$\mathbf{H}_9 = \begin{pmatrix} 4 & 0 \\ 0 & 1 \end{pmatrix}$
$\mathbf{H}_{10} = \begin{pmatrix} 4 & 1 \\ 0 & 1 \end{pmatrix}$	$\mathbf{H}_{11} = \begin{pmatrix} 4 & 2 \\ 0 & 1 \end{pmatrix}$	$\mathbf{H}_{12} = \begin{pmatrix} 4 & 3 \\ 0 & 1 \end{pmatrix}$	$\mathbf{H}_{13} = \begin{pmatrix} 2 & 0 \\ 0 & 2 \end{pmatrix}$
$\mathbf{H}_{14} = \begin{pmatrix} 2 & 1 \\ 0 & 2 \end{pmatrix}$	$\mathbf{H}_{15} = \begin{pmatrix} 1 & 0 \\ 0 & 4 \end{pmatrix}$	$\mathbf{H}_{16} = \begin{pmatrix} 5 & 0 \\ 0 & 1 \end{pmatrix}$	$\mathbf{H}_{17} = \begin{pmatrix} 5 & 1 \\ 0 & 1 \end{pmatrix}$
$\mathbf{H}_{18} = \begin{pmatrix} 5 & 2 \\ 0 & 1 \end{pmatrix}$	$\mathbf{H}_{19} = \begin{pmatrix} 5 & 3 \\ 0 & 1 \end{pmatrix}$	$\mathbf{H}_{20} = \begin{pmatrix} 5 & 4 \\ 0 & 1 \end{pmatrix}$	$\mathbf{H}_{21} = \begin{pmatrix} 1 & 0 \\ 0 & 5 \end{pmatrix}$

Table 3.1: Enumeration of the upper Hermite normal form matrices with determinant ranging from 2 to 5

can be couples of symmetric stop-band curves. When the spectral mask itself enjoys quadrantal symmetry (case (1)), we can consider just one interpolator filters for each couple.

For our experiments, we have chosen minimax 1-D filters with equal stop-band and pass-band ripples. In order to provide some homogeneity in the results, the order of the 1-D filters in the design of the interpolator $H^0(\mathbf{f})$ have been chosen so as to obtain the same ripples exhibited by the 1-D filters in the design of $H^1(\mathbf{f})$.

The overall ripples are related to the ripples of $H^0(\mathbf{f})$, and of the decimated version of $H_1(\mathbf{f})$, in a fashion similar to (1.3),(1.4). Note that, according to the arguments of Section 2.3.6, increasing the index of Λ_i in Λ typically leads to higher ripples relative to the decimated version of $H^1(\mathbf{f})$. This fact is in accordance with our experimental results, where higher decimation ratios correspond (although in a non-linear fashion) to increased amount of the overall ripples.

Finally, note that all the figures of this section represent pass-band curves (solid line) and stop-band curves (dashed line) of real filters (computed according to the definitions of Appendix B) within the square $\mathcal{R}(0.5,0.5)$.

Case 1.

The first example considers a diamond-shaped spectral mask. The pass-band curve is $Par(\mathbf{v}_1|\mathbf{v}_2)$, with $\mathbf{v}_1 = (1/10, 1/20)^T$, $\mathbf{v}_2 = (-1/10, 1/20)^T$, while the stop-band curve is $Par(\alpha\mathbf{v}_1|\alpha\mathbf{v}_2)$ with $\alpha = 3/2$. The definition lattice is $\Lambda = Z^2$ ($\mathbf{C} = \mathbf{I}$). Following the algorithm of Section 2.1, one finds the decimation matrix $\mathbf{A} = \begin{pmatrix} 2 & 1 \\ -2 & 1 \end{pmatrix}$. The frequency response of the shaping filter (before the decimation) $H^1(\mathbf{f})$ is depicted in Fig. 3.4(right), while that of $\hat{H}^1(\mathbf{f})$ (see (2.9)) is depicted in Fig. 3.4(left). Note that $\hat{H}^1(\mathbf{f})$ is periodic on $LAT(\mathbf{A}^{-T})$.

The 1-D filters in the design of $H^1(\mathbf{f})$ were both of length 61; the pass-band and stop-band ripples were $\delta_p = \delta_s = 0.05$. Using the non-factorable implementation, 465 multiplications and 929 sums per input samples are required for the implementation of $H^1(\mathbf{f})$, while exploiting the generalized factorable, such values are reduced to 108 and 117 respectively. Note that the upper Hermite normal form matrix associate to \mathbf{A} is $\begin{pmatrix} 4 & 1 \\ 0 & 1 \end{pmatrix}$, therefore the conditions for the quadrantal-like symmetry of the filter coefficients, studied in Section 2.3.4 are not satisfied. This fact is curious, since the ideal frequency response of Fig. 3.4(right) is actually quadrantly symmetry.

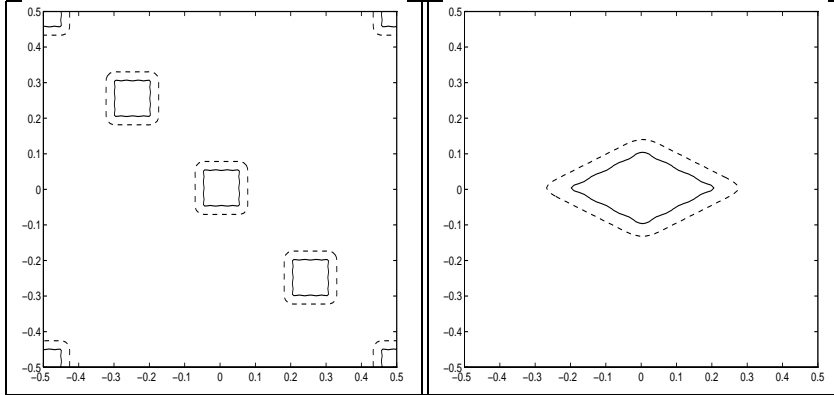


Figure 3.4: Frequency response of $\hat{H}^1(\mathbf{f})$ (left) and of $H^1(\mathbf{f})$ (right) prior to decimation, relative to Case 1.

The frequency responses of the considered filters are shown in Fig. 3.5. Each row of Fig. 3.5 is related to a sublattice $\Lambda_i = LAT(\mathbf{CH}_i)$, where \mathbf{H}_i is indicated in the leftmost column, according to the enumeration of Tab. 3.1. The second and the fourth columns show filters $\hat{H}^1(\mathbf{f})$ and $H^1(\mathbf{f})$ (after decimation on Λ_i) respectively. The third column and the fifth column show $\hat{H}^0(\mathbf{f})$ and $H^0(\mathbf{f})$ respectively. The stop-band region of each filter $\hat{H}^0(\mathbf{f})$ is a maximal rectangle. The sixth column shows the overall frequency response of the IFIR structure.

As noted above, we have kept just one interpolator filter for each couple of symmetrical ones. In plus, due to the quadrantal symmetry of the spectral mask (Fig. 3.4(right)), the IFIR structures relative to a number of couples of sublattices (namely, $(\mathbf{H}_6, \mathbf{H}_7)$, $(\mathbf{H}_{10}, \mathbf{H}_{12})$, $(\mathbf{H}_{18}, \mathbf{H}_{19})$) exhibit a completely symmetrical behaviour, and we have showed only one instance for each such couple.

The quantitative results are summarized in Tab. 3.2. For each sublattice $LAT(\mathbf{CH}_i)$, the lengths N_1^0 and N_2^0 of the 1-D filters used in the design of $H^0(\mathbf{f})$ are reported, together with the overall number of multiplications and of sums per input sample relative to the non-factorable implementation (MNF,SNF) and to the generalized factorable implementation (MGF,SGF). The two rightmost columns of Tab. 3.2 show the pass-band and stop-band ripples δ_p and δ_s of the overall IFIR structure.

In order provide a better understanding of the results (in terms of reduction of MNF and SNF), the upper Hermite normal form matrix associated to each \mathbf{AH}_i (called \mathbf{P} in Tab. 3.2) has been computed. Whenever either $P_{1,1} = 2P_{1,2}$, or \mathbf{P} is diagonal, the condition for the quadrantal-like symmetry of the coefficients of $H^1(\mathbf{f})$ (decimated on $LAT(\mathbf{CH}_i)$) (see Section 2.3.4) is satisfied, and can be exploited for the reduction of the number of multiplications in the non-factorable implementation. Such a profitable contingency is verified in the cases of \mathbf{H}_4 and \mathbf{H}_{14} . In particular, in the case of \mathbf{H}_{14} , the MNF and the SNF are reduced approximately by a factor 5 and 3 respectively by using the IFIR structure.

In Tab. 3.2 we have also reported matrix \mathbf{D} , the basis of the L.D.F.L. containing $LAT(\mathbf{AH})$. As described in Section 2.1.1, decimating the impulse response of $H^1(\mathbf{f})$ on $LAT(\mathbf{CH})$ corresponds to lower computational weight (using the generalized factorable implementation) only if the L.D.F.L. containing $LAT(\mathbf{CH})$ is less dense than the L.D.F.L. containing $LAT(\mathbf{A})$ (in this case, Z^2). In fact, for the cases of \mathbf{H}_3 , \mathbf{H}_8 and \mathbf{H}_{10} such a condition is not verified, and the MGF and the SGF are higher than in the case of the one-stage implementation. Hence, in such cases, the IFIR scheme is not profitable. On the other side, when $\det(\mathbf{D}) > 1$, the IFIR scheme yields computational weight reduction using generalized factorable implementation. For example, in the case of \mathbf{H}_{14} , the MGF and the SGF are reduced approximately by a factor 2.4 and 2.2 respectively.

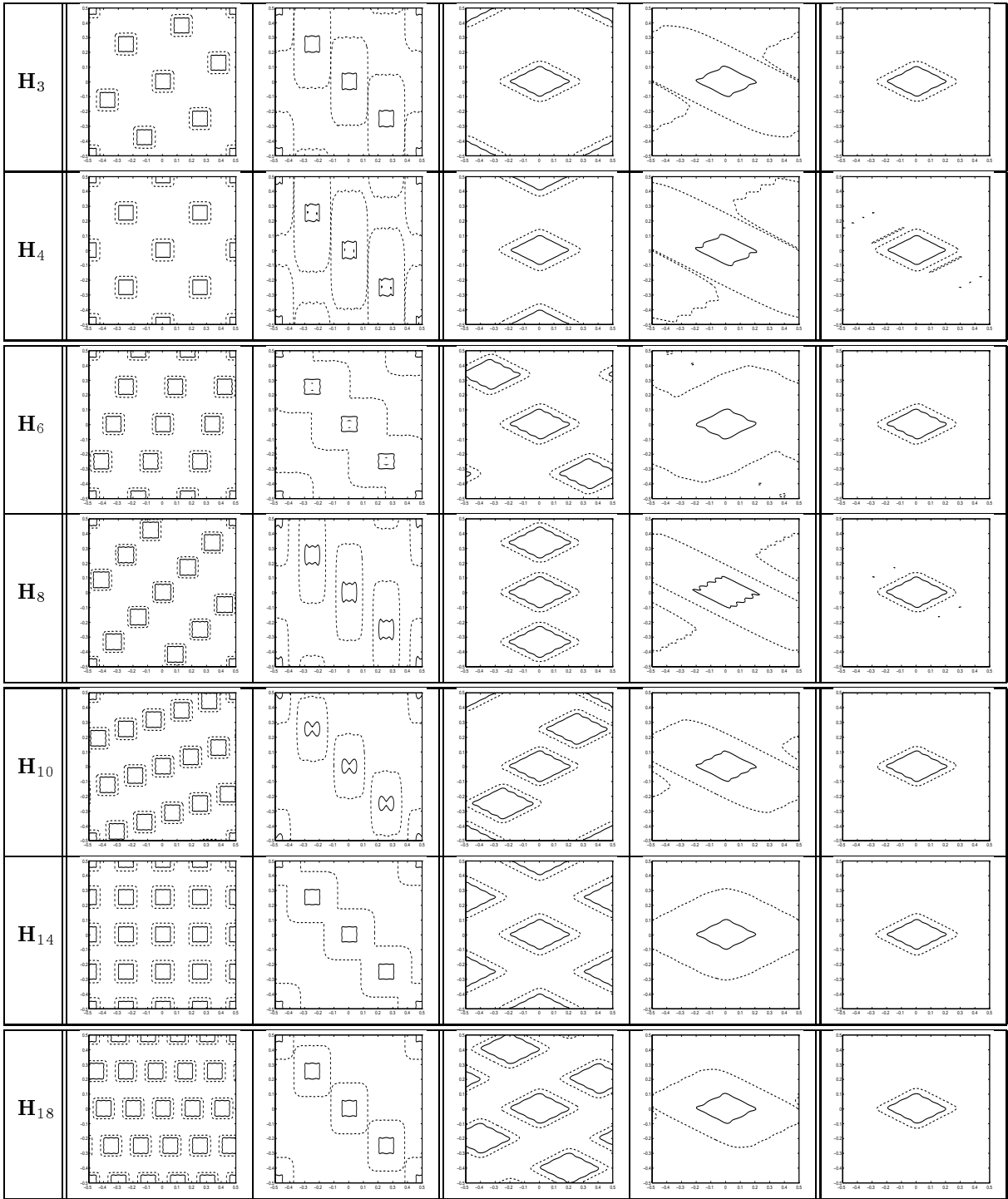


Figure 3.5: Frequency responses of the considered filters - Case 1. Each row of is related to a sublattice $\Lambda_i = LAT(\mathbf{CH}_i)$. Second and fourth column: filters $\hat{H}^1(\mathbf{f})$ and $H^1(\mathbf{f})$ (after decimation on Λ_i). Third and fifth column: filters $\hat{H}^0(\mathbf{f})$ and $H^0(\mathbf{f})$. Sixth column: overall frequency response of the IFIR structure.

	P	D	N_1^0	N_2^0	MNF	SNF	MGF	SMF	δ_p	δ_s
\mathbf{H}_3	$\begin{pmatrix} 8 & 5 \\ 0 & 1 \end{pmatrix}$	$\begin{pmatrix} 1 & 0 \\ 0 & 1 \end{pmatrix}$	21	7	250	499	142	136	0.07	0.04
\mathbf{H}_4	$\begin{pmatrix} 4 & 2 \\ 0 & 2 \end{pmatrix}$	$\begin{pmatrix} 2 & 0 \\ 0 & 2 \end{pmatrix}$	21	5	129	489	70	78	0.06	0.02
\mathbf{H}_6	$\begin{pmatrix} 12 & 9 \\ 0 & 1 \end{pmatrix}$	$\begin{pmatrix} 3 & 0 \\ 0 & 1 \end{pmatrix}$	9	15	171	341	94	95	0.08	0.07
\mathbf{H}_8	$\begin{pmatrix} 12 & 5 \\ 0 & 1 \end{pmatrix}$	$\begin{pmatrix} 1 & 0 \\ 0 & 1 \end{pmatrix}$	39	7	189	376	160	150	0.09	0.02
\mathbf{H}_{10}	$\begin{pmatrix} 16 & 5 \\ 0 & 1 \end{pmatrix}$	$\begin{pmatrix} 1 & 0 \\ 0 & 1 \end{pmatrix}$	25	9	144	286	150	134	0.13	0.06
\mathbf{H}_{14}	$\begin{pmatrix} 4 & 0 \\ 0 & 4 \end{pmatrix}$	$\begin{pmatrix} 4 & 0 \\ 0 & 4 \end{pmatrix}$	15	15	86	256	44	53	0.07	0.02
\mathbf{H}_{18}	$\begin{pmatrix} 20 & 5 \\ 0 & 1 \end{pmatrix}$	$\begin{pmatrix} 5 & 0 \\ 0 & 1 \end{pmatrix}$	21	15	132	262	98	99	0.11	0.05

Table 3.2: Parameters of the considered IFIR structures - Case 1. Matrices \mathbf{P}, \mathbf{D} : see text. N_1^0, N_2^0 =lengths of the 1-D filters used for $H^0(\mathbf{f})$. MNF,SNF = overall number of multiplications and sums required for the non-factorable implementation. MGF,SGF = overall number of multiplications and sums required for the generalized factorable implementation.

Case 2.

In this example, we have considered a narrow oriented spectral mask (see Fig. 3.6(right)). Such filters are employed, for instance, in motion detection algorithms, or for texture discrimination. The pass-band curve is $Par(\mathbf{v}_1|\mathbf{v}_2)$, with $\mathbf{v}_1 = (7/40, 1/8)^T$, $\mathbf{v}_2 = (1/40, -1/40)^T$, while the stop-band curve is $Par(\alpha\mathbf{v}_1|\alpha\mathbf{v}_2)$ with $\alpha = 3/2$. The definition lattice is $\Lambda = Z^2$ ($\mathbf{C} = \mathbf{I}$). In this case, the decimation matrix is $\mathbf{A} = \begin{pmatrix} 7 & 5 \\ -1 & 1 \end{pmatrix}$. The upper Hermite normal form matrix associated to \mathbf{A} is $\begin{pmatrix} 12 & 5 \\ 0 & 1 \end{pmatrix}$, therefore the condition for the quadrantal-like symmetry of the coefficients of $H^1(\mathbf{f})$ is not satisfied in this case either.

Choosing 1-D filters with length equal to 85, the pass-band and stop-band ripples of $H^1(\mathbf{f})$ are 0.07 and 0.04 respectively. Then, for the one-stage implementation, MNF=301, SNF=601, MGF=164 and SGF=157.

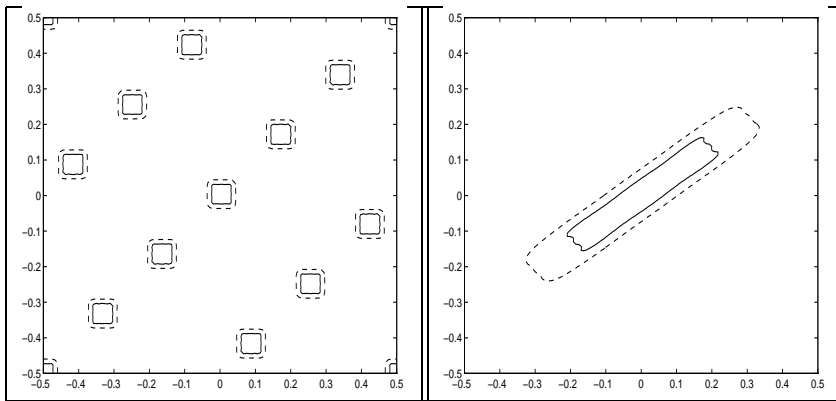
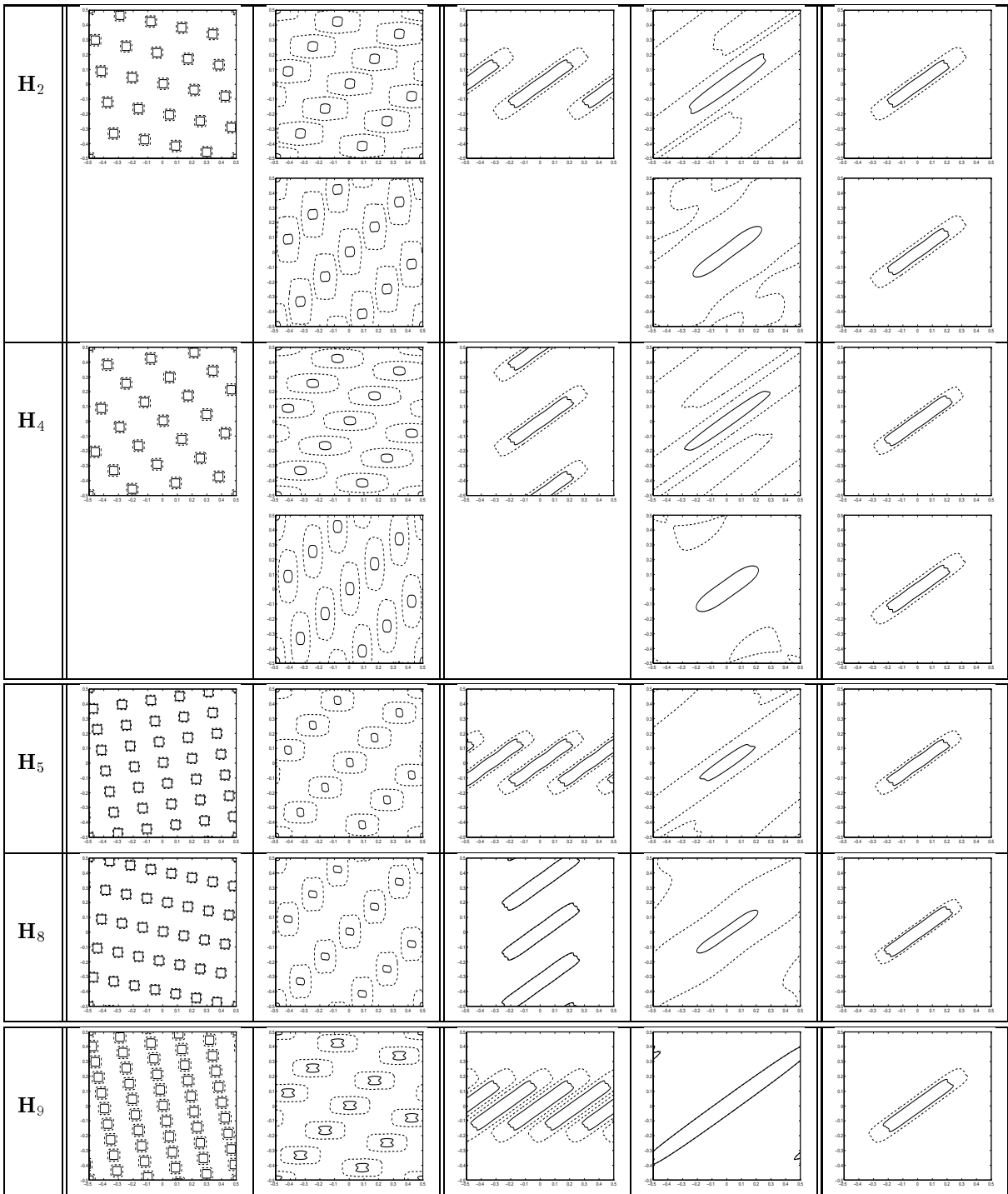


Figure 3.6: Frequency response of $\hat{H}^1(\mathbf{f})$ (left) and of $H^1(\mathbf{f})$ (right) prior to decimation, relative to Case 2.

Fig. 3.7 shows the behaviour of the filters for the different sublattices with index in $\Lambda = Z^2$ ranging from 2 to 5. Note that, corresponding to certain sublattices (namely, $LAT(\mathbf{CH}_2), LAT(\mathbf{CH}_4), LAT(\mathbf{CH}_{15})$), more than one interpolator is found with our algorithm.

The quantitative results are shown in Tab. 3.3. In this example, none of the lattices $LAT(\mathbf{CH}_i)$ satisfies the condition for the quadrantal-like symmetry. In plus, all matrices \mathbf{D} are equal to \mathbf{I} . Hence, adopting the generalized factorable implementation, the IFIR scheme increases the number of OPS's for all of the sublattices of this example. If the non-factorable implementation is used, computational weight reduction is achieved with the IFIR scheme. For example, in the case of \mathbf{H}_2 , little more than one half of MNF and SNF, with respect to the direct one-stage implementation, are required. Higher reduction is gained using less dense sublattices (such as $LAT(\mathbf{CH}_{19})$). However, the ripples of the overall frequency response corresponding to $LAT(\mathbf{CH}_{19})$ are much higher than in the one-stage case. To achieve smaller ripples we should increase the size of the interpolator.



(Continued on next page)

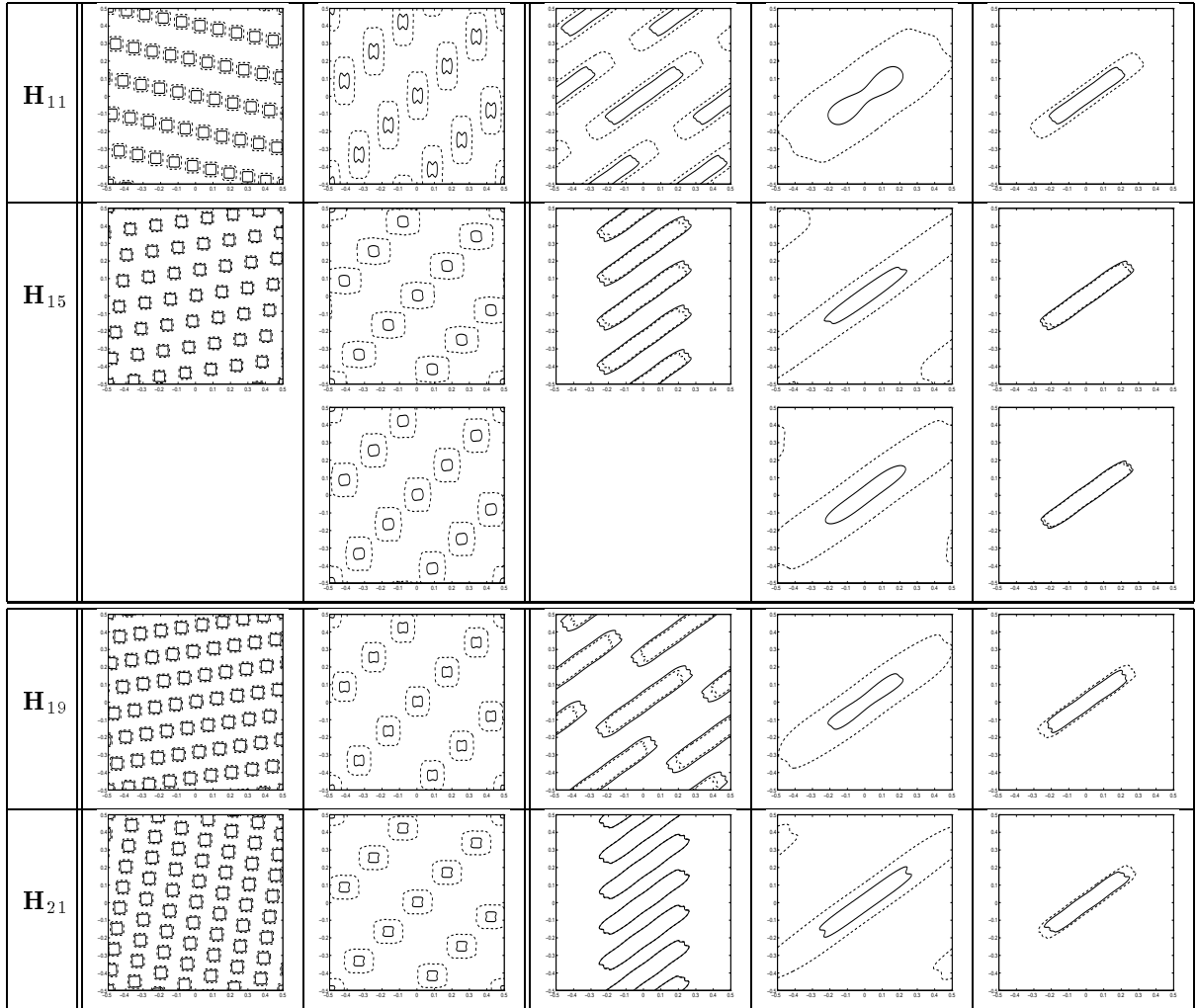


Figure 3.7: Frequency responses of the considered filters - Case 2. Each row of is related to a sublattice $\Lambda_i = LAT(\mathbf{CH}_i)$. Second and fourth column: filters $\hat{H}^1(\mathbf{f})$ and $H^1(\mathbf{f})$ (after decimation on Λ_i). Third and fifth column: filters $\hat{H}^0(\mathbf{f})$ and $H^0(\mathbf{f})$. Sixth column: overall frequency response of the IFIR structure.

	P	D	N_1^0	N_2^0	MNF	SNF	MGF	SMF	δ_p	δ_s
H₂	$\begin{pmatrix} 24 & 5 \\ 0 & 1 \end{pmatrix}$	$\begin{pmatrix} 1 & 0 \\ 0 & 1 \end{pmatrix}$	13	31	166	332	211	176	0.08	0.04
			31	13	166	332	211	176	0.07	0.04
H₄	$\begin{pmatrix} 24 & 17 \\ 0 & 1 \end{pmatrix}$	$\begin{pmatrix} 1 & 0 \\ 0 & 1 \end{pmatrix}$	9	33	162	323	209	174	0.17	0.10
			9	33	162	323	209	174	0.09	0.05
H₅	$\begin{pmatrix} 36 & 5 \\ 0 & 1 \end{pmatrix}$	$\begin{pmatrix} 1 & 0 \\ 0 & 1 \end{pmatrix}$	15	25	115	229	207	160	0.08	0.16
H₈	$\begin{pmatrix} 36 & 29 \\ 0 & 1 \end{pmatrix}$	$\begin{pmatrix} 1 & 0 \\ 0 & 1 \end{pmatrix}$	25	15	115	229	207	160	0.18	0.15
H₉	$\begin{pmatrix} 48 & 5 \\ 0 & 1 \end{pmatrix}$	$\begin{pmatrix} 1 & 0 \\ 0 & 1 \end{pmatrix}$	17	51	111	220	236	176	0.20	0.02
H₁₁	$\begin{pmatrix} 48 & 29 \\ 0 & 1 \end{pmatrix}$	$\begin{pmatrix} 1 & 0 \\ 0 & 1 \end{pmatrix}$	51	17	111	220	236	176	0.12	0.02
H₁₅	$\begin{pmatrix} 48 & 41 \\ 0 & 1 \end{pmatrix}$	$\begin{pmatrix} 1 & 0 \\ 0 & 1 \end{pmatrix}$	33	23	106	211	225	164	0.25	0.20
			23	33	106	211	225	164	0.25	0.20
H₁₉	$\begin{pmatrix} 60 & 17 \\ 0 & 1 \end{pmatrix}$	$\begin{pmatrix} 1 & 0 \\ 0 & 1 \end{pmatrix}$	37	29	104	207	234	162	0.23	0.21
H₂₁	$\begin{pmatrix} 60 & 53 \\ 0 & 1 \end{pmatrix}$	$\begin{pmatrix} 1 & 0 \\ 0 & 1 \end{pmatrix}$	29	37	104	207	234	162	0.28	0.20

Table 3.3: Parameters of the considered IFIR structures - Case 1. Matrices **P**,**D**: see text. N_1^0, N_2^0 =lengths of the 1-D filters used for $H^0(\mathbf{f})$. MNF,SNF = overall number of multiplications and sums required for the non-factorable implementation. MGF,SGF = overall number of multiplications and sums required for the generalized factorable implementation.

Chapter 4

Conclusions

In this work we have proposed an extension to the 2-D case of the idea of Interpolated FIR filters. Several issues that do not have a counterpart in the 1-D case, such as the choice of the subsampling lattice and of the interpolator, have been dealt with. We have considered only spectral supports in the shape of parallelograms, for which Generalized Factorable filters stand as a profitable choice.

The experiments have been done considering both the generalized factorable and the non-factorable implementation of the filters. The results show that with non-factorable filters, good gains (in terms of computational weight reduction) are achievable. Using the generalized factorable implementation, depending on the spectral support shape, IFIR schemes can lead to the reduction of the computational burden in certain cases.

Future work will be led toward a theory of IFIR filters for a generic spectral support.

Appendix A

Some lattice theory basics

In this Appendix we report some notions of lattice theory that are used extensively throughout the work, together with the adopted nomenclature. Section A.1 contains facts already described in the literature. For their proofs, as well as for more details, the reader is addressed to [34],[15],[16],[14]. Section A.2 reports some novel results.

A.1 Lattice theory: background

We will denote vectors by small boldface letters and matrices by capital boldface letters. Their entries are named after the following example:

$$\mathbf{a} \stackrel{\text{def}}{=} (a_1, a_2)^T ; \mathbf{A} \stackrel{\text{def}}{=} \begin{pmatrix} A_{1,1} & A_{1,2} \\ A_{2,1} & A_{2,2} \end{pmatrix} \quad (\text{A.1})$$

Given two sets A and B , we will denote their difference (i.e., the set of elements of A that do not belong to B) as A/B .

We will always deal with square full-rank matrices in this work. Matrix \mathbf{I} is the identity matrix. For the purpose of this section, we assume that the size of the considered matrices is fixed to M .

Given a matrix $\mathbf{V} = (\mathbf{v}_1 | \mathbf{v}_2 | \dots | \mathbf{v}_M)$, we define as $Par(\mathbf{V})$ the parallelepiped $\sum_{i=1}^M \alpha_i \mathbf{v}_i$, $-1 \leq \alpha_i \leq 1$. Given a point \mathbf{u} , we define as $\mathcal{R}(\mathbf{u})$ the parallelepiped with edges parallel to the axes $\{\mathbf{a} : |a_i| \leq |u_i|\}$.

Given a rational number a , $\text{den}(a)$ denotes the least positive integer such that $a \cdot \text{den}(a)$ is integer. Given a rational matrix \mathbf{A} , $\text{den}(\mathbf{A})$ will denote the least positive integer such that $\mathbf{A} \cdot \text{den}(\mathbf{A})$ is an integral matrix. In other words, $\text{den}(\mathbf{A})$ is the least common multiple among $\{\text{den}(A_{i,j})\}$.

Any integral matrix \mathbf{U} such that \mathbf{U}^{-1} is still integral (or, equivalently, such that $|\det(\mathbf{U})| = 1$) is called *unimodular*. Two integral matrices $\mathbf{A}_1, \mathbf{A}_2$ such that $\mathbf{A}_2^{-1} \mathbf{A}_1$ is integral (or, equivalently, such that $\mathbf{A}_1 = \mathbf{A}_2 \mathbf{U}$ with unimodular \mathbf{U}) are called *right-equivalent* or *associated*. For each class of associates, there is just one *Hermite normal form matrix*, i.e. a matrix \mathbf{A} such that

1. \mathbf{A} is upper triangular
2. $A_{i,j} \geq 0$
3. $A_{i,j} < A_{i,i}$ for $1 \leq i < j \leq M$
4. $A_{i,j} = 0$ if $A_{i,i} = 0$

A lattice Λ that admits a basis \mathbf{A} will be denoted as $LAT(\mathbf{A})$. Matrices \mathbf{A}_1 and \mathbf{A}_2 are bases of the same lattice if (and only if) $\mathbf{A}_2^{-1} \mathbf{A}_1$ is unimodular. When dealing with sampling lattices,

we will always assume that they are sublattices of Z^M (i.e., they are *integral* lattices, so that they admit only integral bases).

Let $\Lambda = LAT(\mathbf{B})$ be a sublattice of $\Lambda = LAT(\mathbf{A})$. Then $\mathbf{H} = \mathbf{A}^{-1}\mathbf{B}$ is integral. Term $|\det(\mathbf{H})|$ is called the *index* of Λ in Λ , and is the number of cosets in the quotient group $\Lambda : \Lambda$. Given an elementary cell \mathcal{C} of Λ , the set of points of Λ in \mathcal{C} is a *fundamental period* of Λ [35]. We will denote any generic *fundamental period* of Λ as $P(\mathcal{C}, \Lambda)$.

Let n be an integer. Then the distinct sublattices having index n in $LAT(\mathbf{A})$ are $\{LAT(\mathbf{A}\mathbf{H}_i)\}$, where $\{\mathbf{H}_i\}$ are the Hermite normal forms matrices with determinant equal to n .

We use the following definition for the Fourier transform of a signal $h(\mathbf{a})$ defined on a lattice Λ :

$$H(\mathbf{f}) = \sum_{\mathbf{a} \in \Lambda} h(\mathbf{a}) e^{-j2\pi \mathbf{f}^T \mathbf{a}} \quad (\text{A.2})$$

$H(\mathbf{f})$ is periodic on $\Lambda^* = LAT(\mathbf{A}^{-T})$, where $\mathbf{A}^{-T} \stackrel{\text{def}}{=} (\mathbf{A}^{-1})^T$.

Note that we use term “filter” indicating both its impulse response (denoted by small letter) and its frequency response (denoted by capital letter).

A.2 Some novel results

Consider lattice $\Lambda = LAT(\mathbf{A})$ with integral \mathbf{A} . As described in Section A.1, Λ admits a basis \mathbf{A}^u in Hermite normal form. A geometric interpretation of such a fact in the 2-D case is the following (see Fig. A.1, where $\mathbf{A}^u = \begin{pmatrix} 5 & 3 \\ 0 & 1 \end{pmatrix}$): $(A_{1,1}^u, 0)^T$ is the point of Λ on the horizontal positive half-axis closest to the origin, while $(A_{1,2}^u, A_{2,2}^u)^T$ is the point of Λ in the first quadrant at the left of $(A_{1,1}^u, 0)^T$, which has minimum distance to the horizontal axis (note that no other point of Λ is closer to the horizontal axis). From this geometric standpoint, it is straightforward to argue that the same argument should apply interchanging the role of the horizontal and of the vertical axes. For example, from Fig. A.1 we can find a “dual” basis $\mathbf{A}^l = \begin{pmatrix} 1 & 0 \\ 2 & 5 \end{pmatrix}$. Generalizing such an idea, we can infer that any integral lattice admits a basis \mathbf{A}^l in *lower Hermite normal form*, i.e. such that

1. \mathbf{A}^l is lower triangular
2. $A_{i,j}^l \geq 0$
3. $A_{i,j}^l < A_{i,i}^l$ for $1 \leq j < i \leq M$
4. $A_{i,j}^l = 0$ if $A_{i,i}^l = 0$

The “standard” Hermite normal form matrices thus correspond to the *upper Hermite normal form* matrices.

In what follows, we will deal only with two-dimensional lattices. From our previous geometric arguments, one readily recognizes that, once the upper and the lower Hermite normal form bases \mathbf{A}^u and \mathbf{A}^l of Λ are known, finding a basis of the densest factorable sublattice (D.F.S.), Λ' of Λ (see Fig. A.1) is straightforward:

$$\Lambda' = LAT(\mathbf{D}'), \quad \mathbf{D}' = \text{diag}(A_{1,1}^u, A_{2,2}^l) \quad (\text{A.3})$$

Since Λ' is a sublattice of Λ , it must be $\mathbf{A}^{-1}\mathbf{D}' = \mathbf{H}$ with integral \mathbf{H} . One can see (after some computations) that this condition is equivalent to

$$A_{2,2}^l = k_1 A_{2,2}^u, \quad k_1 A_{1,2}^u / A_{1,1}^u = k_2 \quad (\text{A.4})$$

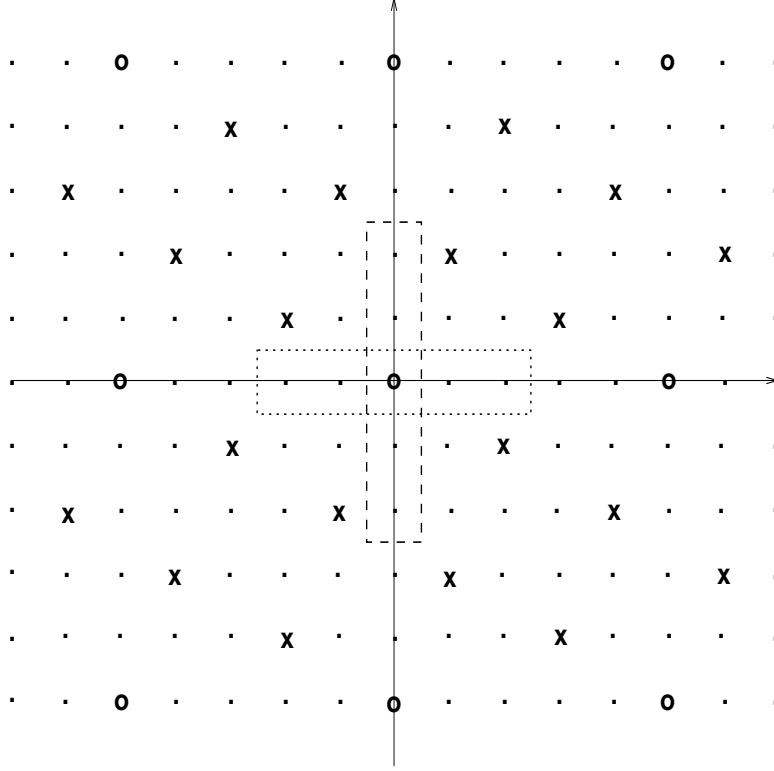


Figure A.1: Lattice Λ (crosses), the L.D.F.L. containing Λ (dots), the D.F.S. of Λ (circles), and the two rectangular elementary cells of Λ (dotted and dashed rectangles).

for some integer k_1, k_2 . In particular, in order for Ψ to be the densest factorable sublattice, k_1 should be the smallest integer for which (A.4) holds true, i.e. $k_1 = \text{den}(A_{1,2}^u/A_{1,1}^u)$. Hence it must be $A_{2,2}^l = A_{2,2}^u \text{den}(A_{1,2}^u/A_{1,1}^u)$. Then, since $\det(\mathbf{A}^u) = \det(\mathbf{A}^l)$, it is $A_{1,1}^u = A_{1,1}^l \text{den}(A_{1,2}^u/A_{1,1}^u)$. This way, we are able to write \mathbf{D}' in terms of \mathbf{A}^u only: $\mathbf{D}' = \text{diag}(A_{1,1}^u, A_{2,2}^u \text{den}(A_{1,2}^u/A_{1,1}^u))$. In particular, the index of Ψ in Λ is $\text{den}(A_{1,2}/A_{1,1})$.

Another important notion is that of the less dense factorable lattice (L.D.F.L.) Ψ that contains Λ . Let $\mathbf{D}'' = \text{diag}(d_1, d_2)$ be a basis of Ψ . Then it must $\mathbf{D}''\mathbf{K} = \mathbf{A}^u$ for some integral matrix \mathbf{K} . This is equivalent to

$$A_{1,1}^u = n_1 d_1, \quad A_{1,2}^u = n_2 d_1, \quad A_{2,2}^u = n_3 d_2 \quad (\text{A.5})$$

for some n_1, n_2, n_3 . Since Ψ is the less dense factorable sublattice among those containing Λ , it must be $d_1 = A_{1,1}^u/\text{den}(A_{1,2}/A_{1,1}) = A_{1,1}^l$ and $d_2 = A_{2,2}^u$. In particular, the index of Λ in Ψ is $\text{den}(A_{1,2}/A_{1,1})$.

Making use of the upper and lower Hermite normal form bases \mathbf{A}^u and \mathbf{A}^l , we can also determine the rectangular elementary cells of Λ centered in the origin with sides pairwise parallel to the axes (throughout this work, we will refer to them with the simple term of “rectangular”). It is easy to prove, starting from our previous geometric observations, that a 2-D integral lattice can admit only two rectangular elementary cells, namely $\mathcal{R}(A_{1,1}^u/2, A_{2,2}^u/2)$ and $\mathcal{R}(A_{1,1}^l/2, A_{2,2}^l/2)$ (see Fig. A.1). In particular, whenever $\text{den}(A_{1,2}/A_{1,1}) = 1$, the two rectangular elementary cells coincide.

Appendix B

Some filter parameter definitions and basic results

This Appendix contains some novel definitions and basic results that are extensively used throughout the work. Only zero-phase filters (i.e., having purely real frequency response) are considered in the following. Unitary sampling period is assumed for the 1-D filters.

The typical minimax parameters of an FIR low-pass filter $h(n)$ are the pass-band and stop-band frequencies f_p and $f_s > f_p$, the pass-band and stop-band ripples $\delta_p \geq 0$ and $\delta_s \geq 0$, and the filter length N . We consider here only low-pass filters approximating unitary steps. Note that quantities f_p and δ_p (as well as f_s and δ_s) are related as

$$\delta_p = \max \{|1 - H(f)|, 0 \leq f \leq f_p\} \quad (\text{B.1})$$

$$\delta_s = \max \{|H(f)|, f_s \leq f \leq 0.5\} \quad (\text{B.2})$$

where $H(f)$ is the frequency response of $h(n)$.

As a matter of fact, f_p, f_s and δ_p/δ_s (or other combinations of the parameters, see [36]) are fixed as *design* parameters. On the other side, when analyzing a given low-pass frequency response (not necessarily optimal), it can be useful to parametrize it in a similar fashion. To this purpose, we introduce here the following definitions of the *analysis* parameters of a given filter $h(n)$:

$$\delta_p = \max \left\{ |1 - H(f_i)|, \frac{dH(f_i)}{df} = 0, |H(f_i)| > 0.5 \right\} \quad (\text{B.3})$$

$$f_p = \min \left\{ f_i : f_i > 0, H(f_i) = 1 - \delta_p, \frac{dH(f_i)}{df} \neq 0 \right\} \quad (\text{B.4})$$

$$\delta_s = \max \left\{ |H(f_i)|, \frac{dH(f_i)}{df} = 0, |H(f_i)| < 0.5 \right\} \quad (\text{B.5})$$

$$f_s = \max \left\{ f_i : f_i < 0.5, H(f_i) = \delta_s, \frac{dH(f_i)}{df} \neq 0 \right\} \quad (\text{B.6})$$

Such definitions, to the author's knowledge, have not been described previously by other authors. Note that the couples (f_p, δ_p) and (f_s, δ_s) identified by (B.4),(B.3) and (B.6), (B.5) respectively, satisfy relations (B.1) and (B.2), unless $\delta_p > 0.5$ or $\delta_s > 0.5$, in which case the filter is unsuitable to any practical purpose. We will assume hereinafter that $\delta_p < 0.5$ and $\delta_s < 0.5$.

The proposed definitions formalize the intuitive notion of parameters $(f_p, f_s, \delta_p, \delta_s)$ for a given frequency response, and suite our purposes when dealing with "well behaved" filters. For example, designing a low-pass minimax filter, by imposing the stop-band and pass-band frequencies, such

two quantities actually coincide with those obtained by applying (B.4) and (B.6) on the resulting frequency response.

We now extend the previous notions to 2-D filters. We start with the case of factorable filters. Given two low-pass FIR filters $h_1(n)$ and $h_2(n)$ (with frequency response $H_1(f)$ and $H_2(f)$), characterized respectively by parameters $(f_{p_i}, f_{s_i}, \delta_{p_i}, \delta_{s_i}, N_i)$, $i = 1, 2$, consider the 2-D filter

$$h(n_1, n_2) = h_1(n_1)h_2(n_2) \quad (\text{B.7})$$

The frequency response of such a filter (periodic on Z^2) is $H(\mathbf{f}) = H_1(f_1)H_2(f_2)$. In the ideal case

$$\delta_{p_1} = \delta_{p_2} = \delta_{s_1} = \delta_{s_2} = 0 \quad (\text{B.8})$$

we have that $H(\mathbf{f}) = 1$ for $\mathbf{f} \in \mathcal{R}(f_{p_1}, f_{p_2})$ and $H(\mathbf{f}) = 0$ for $\mathbf{f} \in \mathcal{R}(0.5, 0.5)/\mathcal{R}(f_{s_1}, f_{s_2})$. In such a case, the *transition region* is “naturally” defined as $\mathcal{R}(f_{s_1}, f_{s_2})/\mathcal{R}(f_{p_1}, f_{p_2})$.

In any practical situation, condition (B.8) is never met, and the intuitive notion of “transition region” needs to be defined precisely. To this purpose, we can adopt a procedure which is reminiscent of the one-dimensional case. We define as *transition region* of a 2-D filter $H(\mathbf{f})$ the region of the elementary cell $\mathcal{R}(0.5, 0.5)$ delimited by the *pass-band curve* $\underline{\mathcal{P}}$ and the *stop-band curve* $\underline{\mathcal{S}}$ (when they are univocally determined), defined as follows:

$$\underline{\mathcal{P}} = \{\mathbf{f} : H(\mathbf{f}) = 1 - \delta_p, \|\nabla H(\mathbf{f})\|^2 \neq 0\} \quad (\text{B.9})$$

$$\underline{\mathcal{S}} = \{\mathbf{f} : H(\mathbf{f}) = \delta_s, \|\nabla H(\mathbf{f})\|^2 \neq 0\} \quad (\text{B.10})$$

where ∇ indicates the gradient operator and

$$\delta_p = \max \{|1 - H(\mathbf{f})|, \|\nabla H(\mathbf{f})\|^2 = 0, H(\mathbf{f}) > 0.5\} \quad (\text{B.11})$$

$$\delta_s = \max \{H(\mathbf{f}), \|\nabla H(\mathbf{f})\|^2 = 0, H(\mathbf{f}) < 0.5\} \quad (\text{B.12})$$

The region \mathcal{P} contained within $\underline{\mathcal{P}}$ is called the *pass-band region* of $H(\mathbf{f})$, while the region of $\mathcal{R}(0.5, 0.5)$ outside $\underline{\mathcal{S}}$ is called the *stop-band region* of $H(\mathbf{f})$. Note that the previous definitions may be easily extended to the case of filters defined on a non-orthogonal lattice. Instead of region $\mathcal{R}(0.5, 0.5)$, any suitable elementary cell of the frequency repetition lattice centered on the origin may be chosen.

It can be interesting checking the proposed definitions for the case of filter $h(n_1, n_2) = h_1(n_1)h_2(n_2)$, where $h_1(n)$ and $h_2(n)$ are low-pass optimal in a minimax sense. Cases of interest for $\nabla H(\mathbf{f}) = \left(\frac{dH_1(f_1)}{df_1} H_2(f_2), H_1(f_1) \frac{dH_2(f_2)}{df_2} \right)^T$ to be null are points such that $\frac{dH_1(f_1)}{df_1} = \frac{dH_2(f_2)}{df_2} = 0$. Extremal interesting points \mathbf{f} thus belong either to region $\mathcal{R}(f_{p_1}, f_{p_2})$ or to region $\mathcal{R}(0.5, 0.5)/\mathcal{R}(f_{s_1}, f_{s_2})$. It is easily seen that

$$\delta_p = \delta_{p_1} + \delta_{p_2} + \delta_{p_1}\delta_{p_2} \simeq \delta_{p_1} + \delta_{p_2} \quad (\text{B.13})$$

while

$$\delta_s = \max \{\delta_{s_1} + \delta_{s_1}\delta_{p_2}, \delta_{s_2} + \delta_{s_2}\delta_{p_1}\} \simeq \max \{\delta_{s_1}, \delta_{s_2}\} \quad (\text{B.14})$$

Consider now the pass-band curve $\underline{\mathcal{P}}$. It is easily seen that $\underline{\mathcal{P}}$ is contained within region $\mathcal{R}(\bar{f}_1, \bar{f}_2)/\mathcal{R}(f_{p_1}, f_{p_2})$, where \bar{f}_1 and \bar{f}_2 are such that $H_1(\bar{f}_1) = (1 - \delta_{p_1} - \delta_{p_2})/(1 + \delta_{p_2})$ and $H_2(\bar{f}_2) = (1 - \delta_{p_1} - \delta_{p_2})/(1 + \delta_{p_1})$. Note that \bar{f}_1 and \bar{f}_2 belong to the transition bands of $H_1(f)$ and $H_2(f)$ respectively (as long as $1 - \delta_{p_1} - \delta_{p_2} > \delta_{s_1}$ and $1 - \delta_{p_1} - \delta_{p_2} > \delta_{s_2}$).

The bandwidth $(\bar{f}_1 - f_{p_1})$ basically depends on i) the pass-band ripple δ_{p_2} and ii) the behaviour of $H_1(f)$ in its transition band. Approximating $H_1(f)$ in its transition band by a linear function, one can show that, for small values of the ripples, $(\bar{f}_1 - f_{p_1})$ can be approximated with $2\delta_{p_2}B_{t_1}$, where $B_{t_1} = (f_{s_1} - f_{p_1})$. Similar considerations apply to bandwidth $(\bar{f}_2 - f_{p_2})$. In what follows, we will always assume that quantities $2\delta_{p_2}B_{t_1}$ and $2\delta_{p_1}B_{t_2}$ are small enough to allow us to approximate $\underline{\mathcal{P}}$ with $\underline{\mathcal{R}}(f_{p_1}, f_{p_2})$.

The case of the stop-band curve $\underline{\mathcal{S}}$ can be treated in a similar fashion. It can be seen that (maintaining that the product δ_p, δ_{s_k} is negligible), if $\delta_{s_1} > \delta_{s_2}$, then $\underline{\mathcal{S}} = \underline{\mathcal{R}}(f_{s_1}, \tilde{f}_2)$, where \tilde{f}_2 is such that $H_2(\tilde{f}_2) = \delta_{s_1}$. Again, approximating $H_2(f)$ in its transition band with a linear function, we have that bandwidth $(f_{s_2} - \tilde{f}_2)$ can be approximated by $(\delta_{s_1} - \delta_{s_2})B_{t_2}$. Also in this case, we will assume that such term is small, allowing us to approximate $\underline{\mathcal{S}}$ by $\underline{\mathcal{R}}(f_{s_1}, f_{s_2})$. Similar considerations hold if $\delta_{s_1} < \delta_{s_2}$.

It is useful now defining the *conventional filter length* of an FIR filter as the number of non-null samples of its impulse response. Such a definition turns out to be profitable when dealing with filters defined on a non-factorable lattice. The conventional order of a filter is approximately proportional to the number of OPS's required in a "direct" implementation.

If N_1 and N_2 are the orders of filters $h_1(n)$ and $h_2(n)$, the conventional order of filter $h(n_1, n_2) = h_1(n_1)h_2(n_2)$ is equal to N_1N_2 , as long as the two 1-D impulse responses do not contain null samples (which turns out to be the case for Nyquist or M -th band filters). In what follows, we will assume that such a condition is met by the considered filters; the results can be easily adapted to the case of impulse responses containing null samples.

Consider now the case of a filter obtained by subsampling an impulse response $\bar{h}(\mathbf{n})$ on a given lattice $\mathcal{L} = LAT(\mathbf{A})$, obtaining $h(\mathbf{Cn})$. Such a filter may be suitable for processing input signals defined on \mathcal{L} , or to obtain different shapes of the pass-band and stop-band regions via a change of basis (see Section 2.1). We define the *conventional length* of a filter defined on a lattice as the number of non-null samples of the filter. Note that, if \bar{N}_c is the conventional length of $\bar{h}(\mathbf{n})$, the conventional length of $h(\mathbf{n})$ is approximately equal to $\bar{N}_c/|\det(\mathbf{A})|$. Assume curve $\underline{\mathcal{S}}$ is contained within some elementary cell of the frequency repetition lattice $\mathcal{L}^* = LAT(\mathbf{A}^{-T})$. The frequency response of the "sampled" filter $H(\mathbf{f})$ is given by

$$H(\mathbf{f}) = \sum_{\mathbf{r} \in P(A)} \bar{H}(\mathbf{f} + \mathbf{r}) \quad (\text{B.15})$$

where $P(Z^2, \hat{\cdot}, *)$ is any Z^2 -period of $\hat{\cdot}, *$.

One could try to analyze $\|\nabla H(\mathbf{f})\|$ in order to obtain parameters $\underline{\mathcal{P}}, \underline{\mathcal{S}}, \delta_p$ and δ_s , according to the previous definitions (B.9)–(B.12). Unfortunately, no general result is to be found, because the position of the zeroes of $\|\nabla H(\mathbf{f})\|$ is unknown *a priori*. However, a simple argument [28] leads to conclude that

$$\delta_p \leq \bar{\delta}_p + (|\det(\mathbf{A})| - 1)\bar{\delta}_s \quad (\text{B.16})$$

and

$$\delta_s \leq |\det(\mathbf{A})|\bar{\delta}_s \quad (\text{B.17})$$

where $\bar{\delta}_p$ and $\bar{\delta}_s$ are the pass-band and stop-band ripples of $\bar{H}(\mathbf{f})$ as in (B.11) and (B.12).

Combining inequalities (B.16) and (B.17), an upper bound for $\delta_p\delta_s$ can be found. Note that in the case of a 1-D filter, one can find a lower bound for the product $\delta_p\delta_s$, too. Let M be the decimation ratio (corresponding to $|\det(\mathbf{A})|$). Then, recalling from (1.2) that the lower bound for $\bar{\delta}_p\bar{\delta}_s$ is a function of the product $\bar{N}\bar{B}_t$ (where \bar{N} is the length of $\bar{h}(n)$ and \bar{B}_t its transition band), and observing that

$$NB_t \simeq \bar{N}\bar{B}_t \quad (\text{B.18})$$

(where $N \simeq \bar{N}/M$ and $B_t \simeq \bar{B}_t M$ are referred to $h(n)$), one maintains that

$$\delta_p\delta_s \geq (\bar{\delta}_p\bar{\delta}_s)^{\text{opt}} \quad (\text{B.19})$$

where $(\bar{\delta}_p\bar{\delta}_s)^{\text{opt}}$ is the product of the pass-band and the stop-band of the optimal filter with length \bar{N} and transition band \bar{B}_t . The determination of similar lower bound relations for the multidimensional case (where relation (1.2) does not apply) is object of current research.

The displacements of the pass-band and stop-band curves $\underline{\mathcal{P}}$ and $\underline{\mathcal{S}}$ (of $H(\mathbf{f})$) with respect to $\bar{\underline{\mathcal{P}}}$ and $\bar{\underline{\mathcal{S}}}$ (of $\bar{H}(\mathbf{f})$) depend mainly on values δ_s and $|\det(\mathbf{A})|$, and on the relative position of the

ripples in the pass-band and in the stop-band regions of $\tilde{H}(\mathbf{f})$. Intuitively, the smaller such values, the “closer” the two curves $\underline{\mathcal{P}}$ and $\underline{\mathcal{S}}$ to $\tilde{\mathcal{P}}$ and $\tilde{\mathcal{S}}$ respectively. In our simplified analysis, we will approximate $\underline{\mathcal{P}}$ and $\underline{\mathcal{S}}$ with $\tilde{\mathcal{P}}$ and $\tilde{\mathcal{S}}$ respectively.

Appendix C

Step response characteristics of ideal filters

In this Appendix we derive a relation between the peak-to-peak ripples of the step response of an ideal low-pass filter $s(n)$ and its sampled version $s(2n)$.

Let $s(n)$ be the impulse response of an ideal low-pass filter with stop-band frequency equal to $0.5/M$ for some even integer M :

$$s(n) = \begin{cases} \frac{\sin\left(\frac{\pi n}{M}\right)}{\pi n} & , \quad n \neq 0 \\ 1/M & , \quad n = 0 \end{cases} \quad (\text{C.1})$$

The output of such filter to a unitary step in the origin is

$$S(n) = \sum_{i=-\infty}^{i=n} s(i) \quad (\text{C.2})$$

Due to the symmetry of $S(n)$, we will consider only its samples for $n \geq 0$. It is easily seen that ripples of $S(n)$ alternate every M samples, and that the peaks of the ripples are for $n = 2kM$ (undershootings) and $n = (2k+1)M$ (overshootings). The difference between the k -th overshooting and its succeeding undershooting, for $k > 0$ is given by

$$D(k) = \sum_{n=(2k-1)M}^{2kM} \frac{\sin\left(\frac{\pi n}{M}\right)}{\pi n} \quad (\text{C.3})$$

Exploiting identity:

$$\sum_{n=0}^M \sin\left(\frac{\pi n}{M}\right) = \cot\left(\frac{\pi}{2M}\right)$$

and inequalities

$$\frac{1}{M} \frac{4k-1}{2k(2k-1) + \frac{1}{4}} < \frac{1}{(2k-1)M+n} + \frac{1}{2kM-n} < \frac{1}{M} \frac{4k+1}{2k(2k-1)}$$

we obtain the following inequalities for $k > 0$:

$$\frac{1}{M\pi} \frac{4k-1}{4k(2k-1) + \frac{1}{8}} \cot\left(\frac{\pi}{2M}\right) < D(k) < \frac{1}{M\pi} \frac{4k-1}{4k(2k-1)} \cot\left(\frac{\pi}{2M}\right) \quad (\text{C.4})$$

Consider now the sampled version of $s(n)$:

$$\bar{s}(n) \stackrel{\text{def}}{=} 2s(2n) = \frac{\sin\left(\frac{\pi 2n}{M}\right)}{\pi n} \quad (\text{C.5})$$

Note in passing that $\bar{s}(n)$ is the ideal low-pass filter with stop-band equal to $0.5/M$. The difference between the k -th overshooting and its succeeding undershooting relative to the step response $\bar{S}(n)$ of $\bar{s}(n)$ is

$$\bar{D}(k) = \sum_{n=(2k-1)M/2}^{kM} \frac{\sin\left(\frac{\pi 2n}{M}\right)}{\pi n}, \quad k > 0 \quad (\text{C.6})$$

Clearly, it is

$$\frac{2}{M\pi} \frac{4k-1}{4k(2k-1) + \frac{1}{8}} \cot\left(\frac{\pi}{M}\right) < \bar{D}(k) < \frac{2}{M\pi} \frac{4k-1}{4k(2k-1)} \cot\left(\frac{\pi}{M}\right) \quad (\text{C.7})$$

From (C.4) and (C.7), the following equalities are derived:

$$2 \left(1 - \frac{1}{32k(2k-1)}\right) \frac{\cot\left(\frac{\pi}{M}\right)}{\cot\left(\frac{\pi}{2M}\right)} < \frac{\bar{D}(k)}{D(k)} < 2 \left(1 + \frac{1}{32k(2k-1)}\right) \frac{\cot\left(\frac{\pi}{M}\right)}{\cot\left(\frac{\pi}{2M}\right)} \quad (\text{C.8})$$

Note that, for $M = 4$ (which is the smallest useful even value for M), it is $\cot\left(\frac{\pi}{M}\right) / \cot\left(\frac{\pi}{2M}\right) = 0.41$, and that such a term monotonically grows with M to its asymptote $1/2$.

Bibliography

- [1] Y. Neuvo, D. Cheng-Yu, and S.K. Mitra. Interpolated finite impulse response filters. *IEEE Transactions on Acoustics, Speech and Signal Processing*, 32:563–570, June 1984.
- [2] P.P. Vaidyanathan. Multirate digital filters, filters banks, polyphase networks, and applications: A tutorial. *Proceedings of the IEEE*, 78(1):56–93, January 1990.
- [3] S.K. Mitra, A. Mahalanobis, and T. Saramäki. A generalized structural subband decomposition of FIR filters and its application in efficient FIR design and implementation. *IEEE Transactions on Circuits and Systems – II: Analog and Digital Signal Processing*, 40(6):363–374, June 1993.
- [4] P.E. Crochiere and L. Rabiner. Optimum FIR digital filter implementation for decimation, interpolation, and narrow-band filtering. *IEEE Transactions on Acoustics, Speech and Signal Processing*, 23(5):444–456, May 1975.
- [5] P.E. Crochiere and L. Rabiner. Further considerations in the design of decimators and interpolators. *IEEE Transactions on Acoustics, Speech and Signal Processing*, 24(4):296–311, August 1976.
- [6] T. Saramäki, Y. Neuvo, and S.K. Mitra. Design of computationally efficient interpolated FIR filters. *IEEE Transactions on Circuits and Systems*, 35:70–87, January 1988.
- [7] D. Pang, L.A. Ferrari, and P.V. Sankar. A unified approach to IFIR filter design using B-spline functions. *IEEE Transactions on Signal Processing*, 39(9):2115–2118, September 1991.
- [8] J.F. Kaiser. Nonrecursive digital filter design using I0-sinh window function. In *Proc. 1974 IEEE Int. Symp. Circuits Syst.*, pages 20–23, April 1974.
- [9] O. Herrmann, L.R. Rabiner, and D.S.K. Chan. Practical design rules for optimum finite impulse response low-pass digital filters. *The Bell System Technical Journal*, 52(6):769–799, July 1973.
- [10] L.R. Rabiner. Approximate design relationships for low-pass FIR digital filters. *IEEE Transactions on Audio and Electroacoustics*, 21(5):456–460, October 1973.
- [11] P.E. Crochiere and L. Rabiner. Interpolation and decimation of digital signals – a tutorial review. *Proceedings of the IEEE*, 69:300–331, March 1981.
- [12] R. Ansari and S. Lee. Two-dimensional non-rectangular interpolation, decimation, and filter banks. In *Proceedings of IEEE ICASSP 88*, New York, April 1988.
- [13] T. Chen and P.P. Vaidyanathan. Recent developments in multidimensional multirate systems. *IEEE Transactions on Circuits and Systems for Video Technology*, 3(2):116–137, April 1993.

- [14] R. Manduchi, G.M. Cortelazzo, and G.A. Mian. Multistage sampling structure conversion of video signals. *IEEE Transactions on Circuits and Systems for Video Technology*, 3(5):325–340, October 1993.
- [15] E. Dubois. The sampling and reconstruction of time-varying imagery with applications in video systems. *Proceedings of the IEEE*, 73:502–522, April 1985.
- [16] G.M. Cortelazzo and R. Manduchi. On the determination of all the sublattices of preassigned index and its application to multidimensional subsampling. *IEEE Transactions on Circuits and Systems for Video Technology*, 3(4):318–320, August 1993.
- [17] R. Bernardini. An efficient algorithm to find lattice chains. Submitted for publication, 1994.
- [18] P. Siohan. 2-D FIR filter design for sampling structure conversion. *IEEE Transactions on Circuits and Systems for Video Technology*, 1:337–350, December 1991.
- [19] Y. Kamp and J.P. Thiran. Chebysev approximation for two-dimensional nonrecursive digital filters. *IEEE Transactions on Circuits and Systems*, 22:208–218, March 1975.
- [20] D.B. Harris and R.M. Mersereau. A comparison of algorithms for minimax design of two-dimensional linear phase FIR filters. *IEEE Transactions on Acoustics, Speech and Signal Processing*, 25(6):492–500, December 1977.
- [21] J. Hu and L. Rabiner. Design techniques for two-dimensional digital filters. *IEEE Transactions on Audio Electroacoustics*, 20:249–257, October 1972.
- [22] A. Biasiolo, G.M. Cortelazzo, and G.A. Mian. Computer aided design of multidimensional FIR filters for video applications. *IEEE Transactions on Consumer Electronics*, 35:290–296, August 1989.
- [23] P. Carrai, G.M. Cortelazzo, and G.A. Mian. Characteristics of minimax FIR filters for video interpolation/decimation. *IEEE Transactions on Circuits and Systems for Video Technology*, August 1994.
- [24] J.H. McClellan. The design of two-dimensional digital filters by transformation. In *Proc. 7th Annual Princeton Conf. Information Sciences and Systems*, pages 257–251, 1973.
- [25] J.S. Lim. *Two-Dimensional Signal and Image Processing*. Prentice-Hall, Englewood Cliffs, New Jersey, 1990.
- [26] D.E. Dudgeon and R.M. Mersereau. *Multidimensional Digital Signal Processing*. Prentice-Hall, Englewood Cliffs, New Jersey, 1984.
- [27] Soo-Chang Pei and Jong-Jy Shyu. Design of 2D FIR digital filters by McClellan transformation and least squares eigencontour mapping. *IEEE Transactions on Circuits and Systems II: Analog and Digital Signal Processing*, 40(9):546–555, September 1993.
- [28] T. Chen and P.P. Vaidyanathan. Multidimensional multirate filters and filter banks derived from one-dimensional filters. *IEEE Transactions on Signal Processing*, 41(5):1749–1765, May 1993.
- [29] A. Knoll. Filter design for the interpolation of highly subsampled pictures. *Signal Processing: Image Communications*, 3:239–248, 1991.
- [30] L. Rabiner and B. Gold. *Theory and Application of Digital Signal Processing*. Prentice Hall, Englewood Cliffs, NJ, 1975.

- [31] G.A. Reitmeir. The effect of analog filtering on the picture quality of component digital television systems. *SMPTE J.*, pages 949–955, October 1981.
- [32] V. Ouvrard and P. Siohan. Design of two-dimensional video filters with spatial constraints. In *Proceedings of EUSIPCO 92*, Brussels, August 1992.
- [33] J.H. Lodge and M.M. Fahmy. K-cyclic symmetries in multidimensional sampled signals. *IEEE Transactions on Acoustics, Speech and Signal Processing*, 31(4):847–860, August 1983.
- [34] M. Newman. *Integral Matrices*. Academic Press, New York, 1972.
- [35] R. Bernardini and R. Manduchi. On the reduction of multidimensional DFT to separable DFT by Smith normal form theorem. *European Transactions on Telecommunications and Related Technologies*, 5(3):377–380, May–June 1994.
- [36] A.V. Oppenheim and R.W. Schaffer. *Digital Signal Processing*. Prentice–Hall, Englewood Cliffs, NJ, 1975.